EVOLUTION OF CLOUD-TO-GROUND LIGHTNING DISCHARGES IN

TORNADIC THUNDERSTORMS

THESIS

WENDY L. SEAMAN, CAPTAIN, USAF

AFIT/GM/ENP/01M-07

DEPARTMENT OF THE AIR FORCE
AIR UNIVERSITY

AIR FORCE INSTITUTE OF TECHNOLOGY

Wright-Patterson Air Force Base, Ohio

APPROVED FOR PUBLIC RELEASE; DISTRIBUTION UNLIMITED.

20010730 046

AFIT/GM/ENP/01M-07

EVOLUTION OF CLOUD-TO-GROUND LIGHTNING DISCHARGES IN

TORNADIC THUNDERSTORMS

THESIS

Presented to the Faculty of the Graduate School of Engineering

of the Air Force Institute of Technology

Air University

Air Education and Training Command

In Partial Fulfillment of the Requirements for the

Degree of Master of Science in Meteorology

Wendy L. Seaman, B.S.,
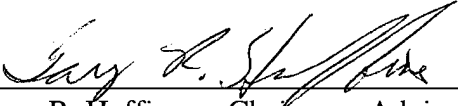
Captain, USAF

February 2000

The views expressed in this thesis are those of the author and do not reflect the official policy or position of the Department of Defense or the U.S. Government.

AFIT/GM/ENP/01M-07

EVOLUTION OF CLOUD-TO-GROUND LIGHTNING DISCHARGES IN

TORNADIC THUNDERSTORMS

Wendy L. Seaman, B.S.,
Captain, USAF

Approved:

Gary R. Huffines	_5 March 2001_
Maj Gary R. Huffines Chairman, Advisory Committee	date
signature	_5 Mar 2001_
Lt Col Glen P. Perram Member, Advisory Committee	date
signature	_05 May 01_
Prof Daniel E. Reynolds Member, Advisory Committee	date

Acknowledgements

"Do, or do not. There is no 'try'. "

Yoda ('The Empire Strikes Back')

If there is one thing I've learned in life, it is that you can do anything if you set your mind to it. As, I've discovered over the last 18 months, going through graduate school and completing a thesis is no exception.

This great feat could not have been accomplished without the unwavering support of AFIT instructors and my classmates. I would like to offer my sincere thanks to my thesis advisor, Major Gary Huffines, who provided guidance and encouragement throughout my research. Without his indepth knowledge of the IDL programming language, I wouldn't have gotten this project completed on time. I would also like to extend my thanks to the members of my thesis committee, LTC Glen Perram and Prof. Dan Reynolds, for their helpful comments and suggestions. Special thanks go to LTC Mark Weadon and the 88th Weather Squadron for sponsoring my research project. Thanks go to all of my classmates who provided the emotional support and humor I needed to maintain my sanity while at AFIT.

I would especially like to thank my husband,   for his love and patience during these months at graduate school. Last but not least, hugs and kisses to   my little ray of sunshine that made even the most stressful days brighter.

Wendy L. Seaman

Table of Contents

List of Figures

List Of Tables

List Of Tables

AFIT/GM/ENP/01M-07

Abstract

Air Force operations are directly impacted by weather on a daily basis. Erroneous forecasts negatively impact mission readiness and consequently cost the government time, in terms of wasted man-hours, and money. Tornadoes complicate the forecasting process even further as they often strike with little or no warning; directly impacting the United States Air Force mission. Advanced forecast lead-time could make a difference to minimize loss to both USAF personnel and assets.

This study examined lightning data from 64 storm events from 1995-2000 in search of unique lightning signatures indicative of tornadic activity. Overall flash rates, percentage of positive flashes, positive and negative peak currents and multiplicity for each case were separated into two categories based on tornado intensity and season of occurrence. The cloud-to-ground lightning data was then scrutinized with the help of time-series analysis. Based on the results of this research, there is little evidence to support the theory that specific lightning trends emerge prior to tornadogenesis.

Due to the inconsistent and unreliable nature of the results, exclusive use of this time-series technique is not recommended for use in operational forecasting. The use of conventional methods, such as radar and/or satellite, used in conjunction with cloud-to-ground lightning flash data may, however, provide insight as to how electrical and physical changes relate to the development of tornadoes within a storm. Intracloud lightning may also provide additional information on tornado development and should be included in future research projects, if the data is available.

EVOLUTION OF CLOUD-TO-GROUND LIGHTNING DISCHARGES IN TORNADIC THUNDERSTORMS

1. Introduction

1.1 Background

Every year, hundreds of tornadoes strike the United States causing unnecessary deaths and producing millions of dollars in damage. These storms often strike with little or no warning and have far-reaching impact on the United States Air Force mission. Advanced forecast lead-time could make a difference to minimize loss to both USAF personnel and assets.

The use of forecasting tools to predict the possible onset of tornadoes is not new in the United States Air Force. E.J. Fawbush and Captain Robert C. Miller of Tinker Air Force Base were reminded just how unpredictable tornadoes can be, during a time when very little was known about these ferocious storms. On March 20, 1948, a devastating tornado ripped through the center of the base destroying over ten million dollars in aircraft in addition to other valuable base assets. After the initial shock had worn off, both forecasters set out to find how the possibility of such a significant event could have been overlooked in their forecast issued earlier that day. After thorough analysis of the storm data, along with comparison of previous storms, Fawbush and Miller discovered that there were common atmospheric conditions present in all of the storm events. Ironically, they had the opportunity to utilize this newly discovered forecasting tool, only five days after the Tinker AFB tornado. However, because precautions were taken early enough, only minimal damage was inflicted on the base.

Within the last 50 years, there has been a growing interest in how the changes in cloud-to-ground lightning relate to the development of severe weather. More specifically, the lightning characteristics associated with tornadic activity have been the focus of many studies. There is some indication from previous work that similar cloud-to-ground (CG) lightning patterns are observed in some storms prior to the onset of tornadoes.

Major David Knapp (1994) addressed this issue while working as a Liaison Officer at the White Sands Missile Range in New Mexico. He examined 264 tornadic thunderstorms and their associated cloud-to-ground lightning characteristics east of the Continental Divide. Knapp (1994) suggested that the examination of Positive Strike Dominated (PSD) storms could be used in nowcasting tornadoes. However, he noted that both Negative Strike Dominated (NSD) and PSD thunderstorms displayed common lightning flash pulsing an hour prior to tornado touchdown with the greatest pulse amplitude seen in PSD storms. Knapp (1994) suggested that forecasters may expect tornado occurrence from PSD storms displaying a rapid flash rate decrease following an earlier peak and lull in cloud-to-ground lightning activity. A shift in polarity from positive to negative CG flashes was also seen ten minutes prior to tornado touchdown indicating a change in the electrical structure of the storms.

Knapp (1994) used this information to create a new technique for nowcasting tornadoes. This method was developed and tested at Offutt AFB, Nebraska, using the lightning data and the Military Weather Advisory (MWA) that Air Force Weather Agency provides to its customers two times a day. The MWA is a synoptic chart depicting a severe weather prognosis for a specific forecast period. High-risk severe weather areas were watched closely for the development of PSD storms. This new

2

technique was found to be very effective in the forecasting of severe weather and tornadoes with a 91% Probability of Detection for all geographic areas regions.

1.2 Problem Statement

Since previous lightning studies have not provided conclusive results, it is clear that further research must be accomplished to determine if there are any CG lightning trends that materialize during severe weather events. If so, determination must be made as to how these trends evolve throughout the life cycle of the storm. Therefore, lightning data from 64 storm events were examined for unique lightning signatures indicative of tornadic activity. This information may be of help in providing Air Force forecasters with another tool for nowcasting tornadoes. More forecast lead-time would allow for additional preparation time, critical to the safety and protection of USAF personnel and assets.

The second objective of this research was not only to verify previously completed research, but also to perform the study on a larger scale than most studies have done in the past. This was accomplished by examining 64 tornadic thunderstorms and their CG lightning characteristics over the continental United States from 1995-2000. With the help of time series analysis, particular attention was paid to flash counts, polarity trends, peak currents, and multiplicity throughout the study period.

1.3 Implications

Air Force operations are directly impacted by weather on a daily basis. Erroneous forecasts negatively impact mission readiness and consequently cost the government time, in terms of wasted man-hours, and money. The unpredictable nature of tornadoes complicates the forecasting process even further.

This research furthers the quest to make the forecasting of tornadoes more predictable by providing new tools to the operational forecaster. The Air Force forecaster has limited time to gather information when putting a forecast together. A streamlined forecasting process will allow forecasters to make warn/no-warn decisions more confidently and efficiently.

1.4 Thesis Organization

This paper is divided up into five chapters in addition to bibliography and appendices follow the body of the paper. Chapter 2 discusses the lightning discharge process, the structure of the National Lightning Detection Network (NLDN) and contains a literature review of previously published work. Chapter 3 discusses methodology used to complete this thesis including details on the thesis objective, scope, and data. Chapter 4 encompasses results and analysis of the project. Finally, Chapter 5 ties the thesis together with conclusions of the research and suggests possible areas for future work.

2. Literature Review

In order to better understand lightning, a review of the types lightning, an explanation of the lightning discharge process, a brief description of the National Lightning Detection Network, and an overview of the history of lightning research will follow .

2.1 The lightning discharge process

What exactly is lightning? Simply put, lightning is a transient, high-current electric discharge whose path length is typically measured in kilometers (Uman, 1987). The lightning discharge is a complex process by which a net charge, negative or positive, is moved from a source region within a cumulonimbus cloud to some point in space, allowing a transfer of charge to take place. Lightning can move from cloud-to-ground, cloud-to-air, cloud-to-cloud, ground-to-cloud, and intracloud. The lightning flash itself is composed of individual strokes, each of which lasts about a millisecond. Worldwide, cloud-to-ground lightning discharges account for over 90 percent of recorded lightning flashes (Uman, 1987). Therefore, it goes without saying that there is abundant cloud-to-ground lightning data available for researchers to analyze. Because of its significance to life and property, in addition to the availability of archived data, cloud-to-ground lightning will be focus of this research project.

Mother Nature likes to maintain equilibrium of electric charge within the environment. The typical fair weather electric field that exists in the environment is on the order of 100 volts/meter. However, this electric field increases significantly within a cumulonimbus cloud at the time breakdown potential is reached. Figure 1 shows the steps of the cloud-to-ground lightning discharge. Once the electric field strength within

the cumulonimbus cloud becomes too great and exceeds the breakdown potential of the

environment, a coronal discharge occurs (Figure 1a) forming a stepped leader.
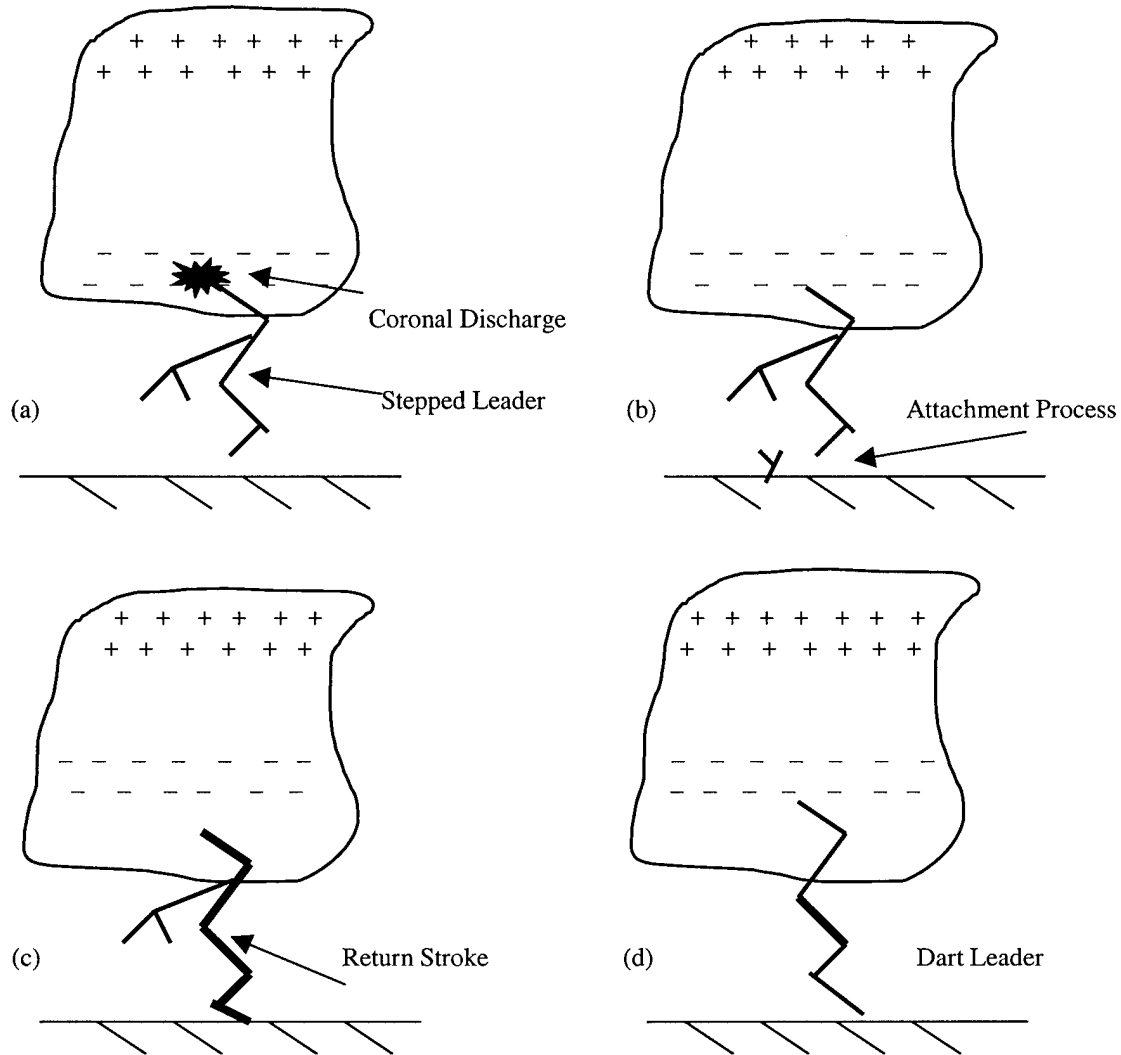
Figure 1. Cloud to ground lightning discharge process (adapted from Uman, 1987).
(a) Coronal discharge occurs when breakdown potential has been reached followed by
movement of a stepped leader from cloud to ground. (b) When stepped leader approaches
the ground, an attachment leader starts upward from the ground, completing the
attachment process. (c) A subsequent return stroke moves charge along the path from the
ground back up to the cloud. (d) The dart leader then moves along the same path from
cloud to ground. The dart leader is sometimes followed by another weaker return stroke.

Following the initial occurrence of the coronal discharge, the stepped leader (Figure 1b) moves down from the base of the cloud toward the ground in distinct steps. Each step is estimated to be 50-100 meters long and is about 1microsecond in duration (Wallace and Hobbs, 1977). As it approaches the ground, the voltage of the stepped leader exceeds the breakdown potential of the surrounding air and an upward-moving discharge is initiated. The joining of the downward moving stepped leader and the upward-moving leader is referred to as the attachment process (Figure 1b). This allows ionized plasma to move from the cloud to the ground through the completed circuit. Immediately following, a return stroke moves up from the ground following the along the previously ionized path allowing a net negative or positive charge down to the earth's surface (Figure 1c). If there is still enough charge remaining in the cloud, a dart leader may propagate downward through the original ionized channel (Figure 1d). As the leader approaches the ground, another return stroke may propagate from the ground to the cloud. Within one lightning flash, this whole process may occur several times in less than a second. The number of strokes that make up a lightning flash is known as multiplicity (Uman, 1987).

2.2 The National Lightning Detection Network (NLDN)

Background information on the National Lightning Detection Network (NLDN) is necessary to understand the source of the lightning data that will be used for this thesis. The NLDN originated in 1987 with the consolidation of three regional networks into one, providing lightning information for the entire United States (Cummins, et al., 1998). Since 1989, this lightning network has provided real-time lightning information on a national level. A system-wide upgrade was warranted in 1994 due to the increasing

demand for improvements in location accuracy, detection efficiency, and estimates of

peak currents of strokes in cloud-to-ground flashes. Cummins et al. (1998) found that

with the upgrade, the NLDN now has an expected location accuracy of 0.5 km over most
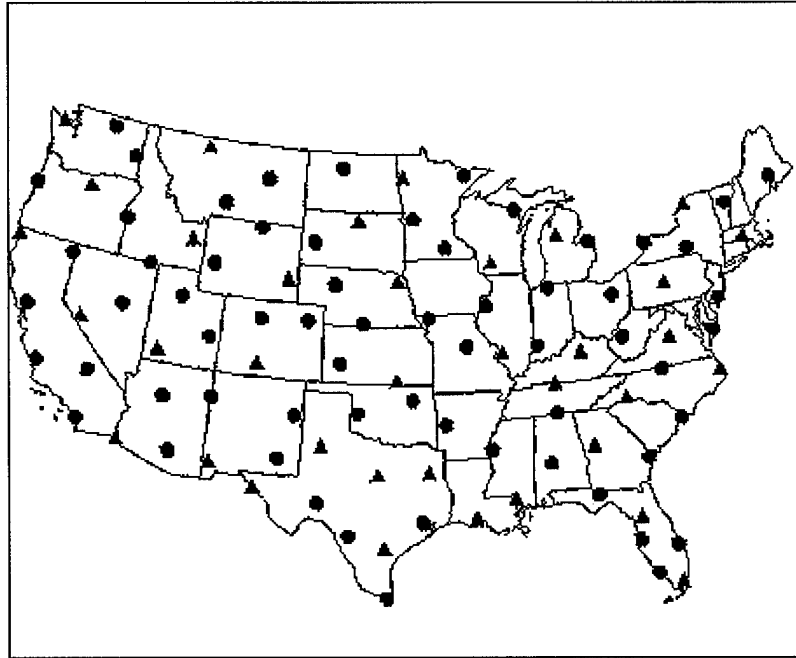
Figure 2. National Lightning Detection Network sensor locations. Triangles represent
IMPACT sensors, and circles show TOA sensors. (Adapted from Cummins, et al., 1998)

of the United States. In addition, overall flash detection efficiency ranges from 80-90%

for events with peak currents greater than 5 kA over the same region. Currently, NLDN

includes 59 TOA (Time of Arrival) sensors used in conjunction with 47 IMPACT

(Improved Accuracy from Combined Technology) sensors. Figure 2 depicts the NLDN

sensor locations throughout the United States.

The TOA sensors (Figure 3) detect lightning discharges by using the time difference

between sensing the arrival of the emitted electric pulse at three stations to create

intersecting hyperbolas that locate the cloud-to-ground lightning flash (Holle and Lopez,

1993). The global positioning system (GPS) is utilized for accurate timing of the
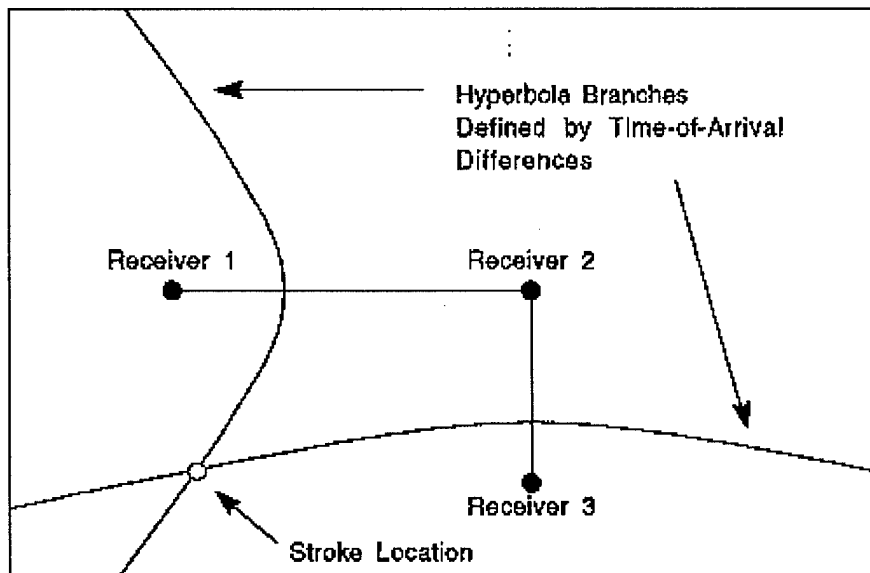
Figure 3. Detection of cloud-to-ground lightning strokes by three time of arrival receivers. (Adapted from Holle and Lopez, 1993)
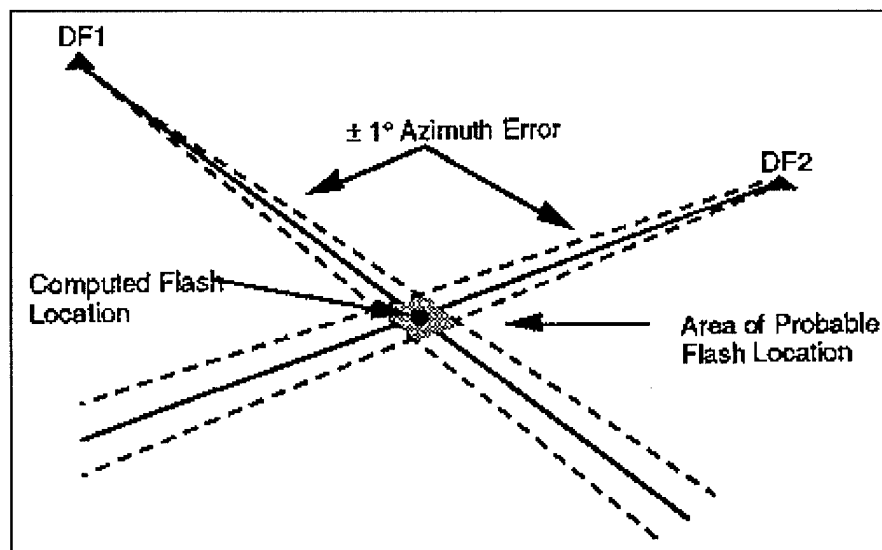
Figure 4. Determination of flash location with two IMPACT sensors. (Adapted from Holle and Lopez, 1993)

lightning pulses. Because TOA sensors are more sensitive than IMPACT sensors, it is also possible for a small percentage of intracloud lightning to be detected. IMPACT sensors (Fig. 4) combine the technology of the magnetic detection finder (MDF) sensors and time of arrival (TOA) sensors mentioned previously. Holle and Lopez (1993) explain that IMPACT sensors measure the electromagnetic field radiated by a lightning flash using two wire loop antennas and a horizontal flat plate antenna which determines the polarity of the CG flash. The radiated magnetic field of a lightning flash induces a current, which is sensed in the wire loops. The current signal measured in the loops is related to the flash's generated magnetic field strength by the cosine of the angle between the loop antenna and the direction to the flash. By comparing the currents from the two loops, a direction to the flash can be determined.

2.3 Early history of lightning research.

Lightning is a phenomenon that has fascinated mankind for thousands of years. Ancient religions and mythologies often depicted lightning as a symbol of punishment, as well as sign of power (Uman, 1987). In the Middle Ages, the focus turned toward ways of protecting structures, especially churches, from lightning strikes. It was thought that the ringing of church bells would disperse the lightning and spare the buildings. Unfortunately, this practice was not successful and claimed many lives in the process.

Benjamin Franklin was one of the first to question the scientific nature of lightning and perform experiments in order to gain a better understanding of this mysterious occurrence. One of Franklin's most famous experiments proved that thunderclouds and therefore, lightning, was indeed electrified. While flying his "electrical kite" during a thunderstorm, sparks jumped from a key tied to the bottom of the kite string to Franklin's

hand. Franklin's later work led to the development of the lightning rod that is still used today to protect buildings and other susceptible structures from lightning strikes (Uman, 1987).

2.4 Recent lightning research

Electromagnetic wave studies by Jones (1951) and Kohl (1962) resulted in a connection between high frequencies of intracloud lightning and tornado occurrence in thunderstorms. Vonnegut (1960) suggested that the electrical energy produced in an intense thunderstorm was strong enough to power a tornado. Further studies by Turman and Tettlebach (1980) proved, through satellite observation, that lightning activity produced by tornadic storms is more intense than that of non-tornadic thunderstorms. Yet some tornadic storms have almost no cloud-to-ground lightning. More recently, Kane (1991) examined electrically active thunderstorms and noted that tornadoes followed a peak in 5-minute lightning rates by 10 to 15 minutes, in addition to a rapid decline in CG rates in conjunction with tornado touchdown. Branick and Doswell (1992), in addition to, Curran and Rust (1992) focused on the structure of tornadic supercells and proposed that low-precipitation supercells are primarily dominated by positive CG flashes. Studies by Seimon (1993), Elson (1993), Knapp (1994) and MacGorman and Burgess (1994), and Perez et al. (1997) suggest that supercell thunderstorms can exhibit unique cloud-to-ground lightning patterns indicative of severe weather.

Branick and Doswell's (1992) study of tornadic thunderstorms over the central and southern Plains focused on storm structure and its relation to observed CG flashes.

11

It was noted that the low precipitation (LP) supercells that tracked through northern

Oklahoma, Kansas, and Nebraska were dominated by a high number of positive CG

flashes. This trend was reversed, however, for the storms that evolved into high

precipitation (HP) supercells. When they evolved, the CG flashes returned to mostly

negative flashes. Similar observations of elevated positive CG rates in LP supercells

have been noted by Curran and Rust (1992) while studying LP supercells that erupted in

Oklahoma on 26 April 1984. They found that 84 percent of CG flashes were positive

with the highest rate of positive CG flashes observed during the splitting and merging

phase of the LP supercells. Overall CG polarity reversed to negative 15-20 minutes prior

to tornado touchdown and remained as such throughout the remainder of the tornadic

phase of the supercells.

More recently, Seimon (1993) studied CG lightning patterns in the deadly Plainfield,

Illinois tornado of 28 August 1990. This F5 tornado was spawned from a thunderstorm

that exhibited unusual CG activity about two hours prior to tornado development.

Several distinct trends emerged within the timeline of the study. Seimon (1993) noted

very high peak current values of positive CG flashes along with very low negative values

during the time prior to tornadogenesis. In addition, CG activity was significantly

reduced within twenty minutes of tornado touchdown and intensification. A subsequent

reversal in CG flashes from positive to negative was observed in conjunction with

tornado touchdown. Another notable trend was that following polarity reversal, positive

peak current amplitudes declined from +100 kA to +38 kA while the negative peak

current amplitudes increased from +20 kA to +40 kA. Spacial analysis showed that at the

time of maximum tornado intensity, all detected CG lightning flashes were concentrated

within a few meters of the tornado. Data analyzed by Seimon (1993) showed a good correlation between maxima in damage severity and maxima in tornado-proximity flash rate along with percentage of total flash count. He also stated that this correlation should be viewed cautiously as the nature of the Fujita scale used in the assessment is highly subjective.

In a study of 14 thunderstorms in Indiana on 2 June 1990, Elson (1993) examined the relationship between lightning intensity and the onset of severe weather. His method of comparison counted the number of minutes CG lightning activity that exceeded a threshold rate of 300 strikes per hour. This rate was selected because it best represented periods of high CG lightning activity in the storms. His results showed that tornadoes typically occurred during periods of low to moderate cloud-to-ground lightning activity. Elson (1993) defined moderate CG activity as 100-300 strikes per hour and low activity as less than 100 CG strikes per hour. His finding is in agreement with previous work done by MacGorman et al. (1989) and Maier and Krider (1982).

Elson (1993) also studied the spatial relationship between severe weather occurrences and lightning centroids. Storm relative locations of severe weather occurrences with respect to the approximate lightning centroid (center of lightning activity) were plotted. It was found that severe weather favored an area a few miles west of the center of CG activity although Elson (1993) noted a considerable amount of variability. Finally, a limited number of severe weather occurrences were evident in the southeast quadrant of the lightning activity.

In an attempt to find a correlation between cloud-to-ground lightning flashes and tornadic thunderstorms, Knapp (1994) studied lightning data from 264 tornadic

thunderstorms east of the Continental Divide. Time-series analysis of five-minute flash rates and percentage positive of lightning flashes showed that specific trends in cloud-to-ground lightning were evident in tornadic thunderstorms. Knapp (1994) found that well defined peak-lull-peak flash rates were exhibited for positive strike dominated (PSD) storms with the highest pulse amplitudes seen twenty minutes prior to tornado occurrence. Further, in PSD storms, he noted a polarity shift to negative CG flashes about the time of the initial tornado report. Results of his study allowed Air Force Weather Agency (AFWA) to develop a new technique for nowcasting severe storms and tornadoes throughout the United States. High-risk severe weather areas were watched closely for the development of PSD storms improving the forecast accuracy of potentially severe storms.

MacGorman and Burgess (1994) studied positive CG lightning tendencies of fifteen tornadic storms in the Central Plains and Midwest. Of the fifteen storms studies, four maintained a dominant positive polarity throughout the life of the storm. The remaining eleven storms maintained a positive flash polarity early, but then reversed polarity to negative as they progressed. It was noted that most of the tornadoes occurred in storms dominated by positive CG flashes. The most intense tornadic activity began after a reduction in positive CG flashes from their peak values. MacGorman and Burgess (1994) found this especially true when maximum flash rates exceeded 1.5 flashes per minute. Furthermore, a lull in CG flashes was observed in between polarity reversal of the CG flashes from positive to negative. This occurred sometimes as long as 40-100 minutes after the positive ground flash rates decreased from their peak. It was during this interval that the most intense tornado activity sometimes began. The authors caution the reader of

14

the one-way nature in the findings. Although severe weather has been observed in storms dominated by positive CG flashes, it has also been observed in storms dominated by negative CG flashes. On the other hand, storms dominated by positive CG flashes for an extended period of time produced severe weather in almost all cases. Only a small percentage of negative CG dominated storms resulted in severe weather.

In a study of lightning characteristics associated with violent tornadoes, Perez et al. (1997) analyzed CG lightning patterns in 42 tornadic thunderstorms that occurred between January, 1989 and November, 1992. As with previous studies, the authors found that there were common lightning flash patterns throughout the time of study. Specifically, the period of time encompassed 30 minutes prior, during, and 30 minutes after the tornadoes' lifetime. First, Perez et al. (1997) noted that 31 of the storms exhibited a local peak in their cloud-to-ground flash rate 15-20 minutes preceding tornado touchdown. Twenty of these storms displayed a decrease in cloud-to-ground activity in conjunction with tornado touchdown. Unlike MacGorman and Burgess' study of 1994, only a small number of storms, 6 out of 42, reversed predominate polarity from positive to negative. It was found that the most intense and long-lived tornadoes were spawned from storms discharging a majority of the positive CG flashes. Perez et al. (1997) contend that flash rate analysis should not be used exclusively to predict the occurrence of tornadoes. However, the authors do suggest CG flash rate trends, used in conjunction with Doppler radar, may be of help in identifying storms which have the potential to produce tornadoes.

3. Methodology

3.1 Overview

The question still remains as to the validity of claims made by previous researchers regarding the trends of CG lightning flashes and possible tornadic activity. Lightning data from various storm events were examined in this study for unique lightning signatures indicative of tornadic activity. This information may be of help in providing Air Force forecasters with another tool for nowcasting tornadoes, increasing critical lead-time to warn customers.

Research completed in the past has been limited in terms of number of tornadic storms examined over the course of study. This study encompassed data from 64 storm events for a 6-year period from 1995 to 2000. Most scientists, such as Kane (1991), Seimon (1993), MacGorman and Burgess (1994), have focused their attention on a very small geographic region within their investigational surveys. This research project examined the lightning characteristics of tornadic thunderstorms from 28 states, primarily east of the Rocky Mountains.

The first step in gathering the CG lightning data was to use IDL (Interactive Data Language) programming language to process the lightning data from the NLDN provided by Global Atmospherics, Inc. of Tucson, Arizona. The lightning data were saved to separate text files for easy manipulation and analysis at a future time. Next, Microsoft Excel was used to create several new files which stored the average peak currents, average multiplicity, and flash counts for both negative and positive polarity flashes. SPSS for Windows was utilized to break the data into smaller components so that it could be observed and graphed more carefully. SPSS was chosen, among other statistical

packages, due to its ease in importing data from other files and performing statistical

analysis on it. SPSS also has the distinct advantage of editing graphs after they have

been created allowing for flexibility in modifications at a later time

3.2 Scope

3.2.1 Storm events

A total of seventy-eight tornado events from 1995 thorough 2000 were

randomly selected from the National Climatic Data Center storm event database.

However, some of the cases were omitted from the analysis portion of the thesis due to

the lack of lightning data. The National Climatic Data Center web-site (NCDC, 1999)

contains an extensive database of storm reports from all over the United States.

Table 1. Storm events list.

Case	Date	Start time	Stop time	Start location	Stop location	Storm	Storm
#	MM/DD/YY	HH:MM:SS	HH:MM:SS	LAT/LON	LAT/LON	Intensity	Location
1	5/18/95	17:42:00	17:42:00	38.25N/90.18W	38.32N/90.15W	F1	Mayestown, IL
3	11/11/95	16:30:00	16:30:00	30.8N/84.32W	30.8N/84.32W	F1	Nickleville, GA
4	3/18/96	23:30:00	23:40:00	31.46N/87.9W	31.53N/87.78W	F1	Jackson Airport, AL
5	7/30/96	20:10:00	20:25:00	39.6N/80.9W	39.55N/80.72W	F1	Paden City, WV
6	10/26/96	19:05:00	19:07:00	45.01N/96.67W	45.06N/96.65W	F1	Revillo, SD
7	5/27/97	20:07:00	20:25:00	30.9N/97.58W	30.87N/97.58W	F1	Prairie Dell, TX
8	6/22/97	21:28:00	21:33:00	44.58N/97.2W	44.58N/97.2W	F1	Lake Norden, SD
10	5/7/98	22:19:00	22:25:00	36.35N/80.62W	36.35N/80.57W	F1	Level Cross, NC
11	6/27/98	23:30:00	23:35:00	39.93N/81.98W	39.92N/81.97W	F1	Zanesville, OH
12	8/25/98	6:00:00	6:00:00	41.83N/86.25W	41.82N/86.22W	F1	Niles, MI
13	4/8/99	19:36:00	19:46:00	40.62N/95.12W	40.73N/95.03W	F1	College Springs, IA
14	5/4/99	21:35:00	21:55:00	38.38N/97.5W	38.51N/96.93W	F1	Marion, KS
15	6/26/99	2:55:00	2:55:00	40.9N/102.8W	40.9N/102.8W	F1	Crook, CO
17	1/3/00	12:22:00	12:25:00	36.22N/92.18W	36.23N/92.15W	F1	Jordan, AR
19	2/14/00	23:15:00	23:25:00	43.35N/112.12W	43.4N/112.06W	F1	Shelley, ID
21	3/7/95	9:16:00	9:20:00	32.06N/91.38W	32.06N/91.38W	F2	Newellton, LA
22	5/18/95	22:30:00	22:35:00	36.98N/86.43W	36.98N/86.43W	F2	Bowling Green, KY
23	6/8/95	22:59:00	23:25:00	35.18N/100.65W	35.23N/100.62W	F2	Mclean, TX
25	7/13/96	4:45:00	5:15:00	39.8N/104.4W	39.65N/104.21W	F2	Strasburg, CO
26	10/26/96	22:10:00	22:15:00	46.32N/95.36W	46.52N/95.43W	F2	Henning, MN

Table 1 (continued). Storm events list.

Case #	Date MM/DD/YY	Start time HH:MM:SS	Stop time HH:MM:SS	Start location LAT/LON	Stop location LAT/LON	Storm Intensity	Storm Location
28	7/3/97	22:05:00	22:15:00	42.16N/73.22W	42.21N/73.15W	F2	Monterey, MA
29	7/16/97	20:38:00	20:40:00	45.11N/89.46W	45.06N/89.52W	F2	Merrill, WI
30	4/15/98	0:43:00	0:49:00	38.42N/89.08W	38.46N/89.01W	F2	Cravat, IL
31	6/23/98	0:25:00	0:36:00	41.48N/97.3W	41.55N/97.21W	F2	Columbus, NE
32	6/27/98	0:46:00	0:57:00	42.98N/93.43W	43.06N/93.38W	F2	Thornton, IA
33	1/21/99	21:57:00	22:00:00	35.13N/92.15W	35.16N/92.11W	F2	Naylor, AR
34	5/4/99	20:06:00	20:21:00	32.38N/94.88W	32.41N/94.70W	F2	Kilgore, TX
35	8/8/99	12:28:00	12:40:00	41.0N/72.51W	41.0N/72.46W	F2	Mattituck, NY
36	8/11/99	18:41:00	18:55:00	40.73N/111.87W	40.73N/111.87W	F2	Salt Lake City, UT
37	1/3/00	19:40:00	20:00:00	34.18N/89.52W	34.38N/89.26W	F2	Paris, MS
38	2/13/00	23:38:00	0:08:00	34.88N/91.98W	34.83N/91.68W	F2	Furlow, AR
39	2/14/00	6:39:00	6:42:00	31.31N/83.63W	31.33N/83.61W	F2	Crosland, GA
40	5/7/95	21:10:00	21:20:00	33.51N/97.53W	33.8N/97.43W	F3	Sunset, TX
42	11/11/95	9:10:00	9:30:00	32.52N/90.40W	32.55N/90.10W	F3	Flora, MS
43	5/26/96	21:45:00	22:15:00	37.63N/100.65W	37.86N/100.4W	F3	Sublette, KS
45	7/19/96	19:42:00	19:45:00	39.5N/76.98W	39.48N/76.95W	F3	Gamber, MD
46	3/29/97	6:10:00	6:30:00	35.05N/85.31W	35.05N/85.18W	F3	Chattanooga, TN
47	7/2/97	0:30:00	0:50:00	38.85N/84.18W	38.81N/84.06W	F3	Moscow, OH
48	9/18/97	23:15:00	23:25:00	46.06N/94.05W	46.05N/93.85W	F3	Lastrup, MN
50	5/31/98	0:50:00	1:10:00	39.75N/79.08W	39.73N/78.96W	F3	Salibury, PA
51	8/23/98	23:30:00	23:44:00	45.01N/87.33W	45.00N/87.21W	F3	Egg Harbor, WI
52	1/21/99	0:05:00	0:16:00	35.65N/91.43W	35.76N/91.36W	F3	Naylor, AR
53	4/8/99	20:16:00	20:23:00	41.15N/94.78W	41.25N/94.70W	F3	Massena, IA
55	10/13/99	21:00:00	21:10:00	39.6N/82.98W	39.61N/82.95W	F3	Circleville, OH
56	1/3/00	22:06:00	22:12:00	37.71N/87.18W	37.76N/87.12W	F3	Rome, KY
57	1/3/00	20:00:00	20:10:00	34.38N/89.25W	34.6N/89.08W	F3	Pinedale, MS
59	5/13/95	21:18:00	22:15:00	41.0N/91.0W	41.0N/91.0W	F4	Niota, IL
60	5/27/95	0:22:00	0:52:00	42.06N/94.9W	42.58N/94.83W	F4	Carroll, IA
61	5/29/95	0:06:00	1:24:00	42.00N/73.00W	42.00N/73.00W	F4	Egremont, MA
62	4/14/96	0:39:00	1:22:00	35.93N/92.1W	36.2N/91.72W	F4	Sylamore, AR
63	5/28/96	22:42:00	23:08:00	38.1N/85.73W	38.05N/85.49W	F4	Brooks, KY
64	1/24/97	23:00:00	23:12:00	35.78N/86.5W	35.83N/86.38W	F4	Murfreesboro, TN
65	3/1/97	0:20:00	1:00:00	35.76N/90.18W	35.95N/89.72W	F4	Lennie, AR
66	5/27/97	21:50:00	22:00:00	30.36N/98.01W	30.33N/97.98W	F4	Lakeway, TX
68	4/16/98	21:50:00	22:15:00	35.21N/88.01W	35.20N/87.63W	F4	Clifton, TN
70	4/3/99	22:01:00	22:20:00	32.58N/93.75W	32.75N/93.6W	F4	Bossier City, LA
71	4/8/99	20:23:00	22:40:00	41.25N/94.71W	41.48N/94.47W	F4	Bridgewater, IA
72	5/11/99	23:05:00	23:45:00	30.68N/99.1W	30.65N/99.0W	F4	Loyal Vly, TX
73	6/6/99	20:20:00	20:30:00	48.6N/97.78W	48.68N/97.85W	F4	Crystal, ND
74	7/18/96	0:05:00	1:28:00	43.7N/88.62W	43.72N/88.38W	F5	Oakfield, WI
75	5/27/97	20:40:00	20:53:00	30.82N/97.62W	30.77N/97.67W	F5	Jarrell, TX
76	4/8/98	0:52:00	1:28:00	33.38N/87.23W	33.58N/86.86W	F5	Oak Grove, AL
77	4/16/98	22:15:00	23:05:00	35.26N/87.58W	35.43N/87.20W	F5	Deerfield, TN
78	5/3/99	0:12:00	0:30:00	35.3N/97.60W	35.37N/97.45W	F5	Moore, OK

Information provided includes location, date, magnitude, path length and width of the tornadoes, in addition to fatalities and storm damage in dollars. Storm events were selected throughout the year without regard to geographical preference. Storms examined have produced tornadoes with intensities varying from F1-F5 intensity on the Fujita scale (Fujita, 1981). Table 2 breaks down the intensity levels of the Fujita scale. Because of the greater frequency of weaker tornadoes, the database for weaker tornadoes is much more extensive than that of violent tornadoes. Lightning characteristics were also examined based on seasonal variations. Table 3 shows how the seasons were divided between months of the year.

Table 2. Fujita Scale for tornadoes (adapted from Fujita, 1981). Miles per hour on table refers to wind speed.

Scale	Category	Miles/Hr	Damage
F0	Weak	40-72	light: tree branches broken
F1	Weak	73-112	moderate: trees snapped, window broken
F2	Strong	113-157	considerable: large trees uprooted, weak structures destroyed
F3	Strong	158-206	severe: trees leveled, cars overturned, walls removed from buildings
F4	Violent	207-260	devastating: frame houses destroyed
F5	Violent	261-318	incredible: homes stripped from concrete slabs, asphalt lifted from roads

Table 3. Seasonal breakdown of months used in analysis.

Spring	Summer	Fall	Winter
March	June	September	December
April	July	October	January
May	August	November	February

3.2.2 Limitations of the data

There are two main areas of data limitation that have been taken into account in this research project. These include determination of tornado intensity and selection of geographical area size to be included in study.

Determination of tornado intensity is very subjective. The experience of the National Weather Service surveyor plays a large part in how each tornado is classified. Based on the Fujita Scale, tornadoes are classified based on how much damage they cause. Of course, a tornado that moving through open country is going to produce less damage than a tornado that plows into a highly populated and developed area. Finally, there is often wind damage from straight-line winds or downbursts associated with severe thunderstorms. Tornado damage has to be separated from other wind damage before a valid assessment can be made.

Unfortunately, it is impossible to say exactly where each CG lightning flash originates for each storm. Therefore, it is difficult to select the size of geographical area that best suits the study. Too large of an area might include unwanted lightning data from non-tornadic storms. On the other hand, too small of an area may miss crucial data associated with the tornadic storms. Not all flashes associated with the tornadoes are going to necessarily be found within the confines of the tornado path. It is possible that the lightning from such storms may originate miles away from the actual tornado.

3.3 Examination of lightning data

3.3.1 Programs utilized

The first program written, **readfile.pro**, accessed the NLDN lightning data stored on the local server at AFIT and saved it to a designated file for each individual storm

event. The computer code for **readfile.pro** can be referenced in Appendix A. Lightning data was saved in both ASCII and binary format for thunderstorms that occurred within a region surrounding the tornado path. In order to enlarge the research area, one degree was added to the minimum and maximum latitude and longitude of the tornado path, taking into consideration that 1 degree of latitude/longitude is approximately equal to 60 nautical miles. Because average movement of thunderstorms was assumed to be approximately 25 knots, a 4-hour block of lightning data was used so lightning data could be examined from the beginning of thunderstorm development until its dissipation. Output included day, time, peak current (including polarities), and multiplicity for each lightning flash.

The program, **histogramdata.pro,** read data from the previously created files from the **readfile** program and calculated average positive and negative flash count, peak current, and multiplicity for a time increment specified by the user. The computer code for **histogramdata.pro** can be referenced in Appendix A. If data within the **readfile.pro** file existed, **histogramdata.pro** isolated positive and negative flash data and placed it into appropriate bins based on how long after the reference start time the flash occurred. The reference times were chosen to be within one hour of the reported tornado occurrence.

Flashes with peak currents greater than 10 kA were considered to be positive CG flashes while flashes with peak currents less than 0 kA were considered to be negative. It should be noted that positive CG flashes less than 10 kA were not used in this research project. Due to the increased sensitivity in the NLDN since the 1994 upgrade, many discharges with peak currents between 5 and 15 kA are now detected. As suggested by

Cummins et al. (1998), it is likely that not all of these are CG discharges, and for that reason, positive peak currents less than 10 kA are considered to be cloud discharges.

A variable, **dt,** which represented change in time (minutes), was created to allow the user the flexibility to change the size of the bin based on how large a time increment was desired. In other words, **dt** could be adjusted based on how long of a time average (in minutes) was required. Once the positive and negative flash data were separated and placed into the appropriate bins, a counter summed up the number of positive and negative flashes in addition to summing the peak current and multiplicity of each type of flash. Finally, average CG flash count, peak current, and multiplicity, both for positive and negative flashes were calculated for each bin and the results sent to individual text files. The creation of the text files allowed the user to import the data into any type of spreadsheet and/or statistical package for future analysis.

3.3.2 Statistical manipulation of data

Microsoft Excel was used to convert the text files into spreadsheets for each of the lightning data categories to further manipulate the data. In addition to the categories of data listed above, an additional file was created for percentage of positive flashes. This thesis examines overall flash rates, percentage of positive flashes, average positive and negative peak currents, and multiplicity for each case.

Hourly flash rates for all CG lightning flashes were calculated in a way similar to that of Kane (1991). The hourly rate was calculated by taking the number of CG flashes within the 2-minute interval preceding the current time and multiplying it by 30. In essence, the hourly rate is an extrapolated value based on the 2-minutes averages and gives a projection of strikes for the next hour.

A summary of averages was calculated for all storms based on intensity and season for one hour prior and one hour after tornado occurrence. For each category of intensity or season, Microsoft Excel was used to calculate the averages of the desired lightning characteristics for the time period of interest. The example shown in Table 4 is based on the data for F5 tornadoes in the hour preceding touchdown. First, the flash count was averaged for each two-minute time increment leading up to tornado start for each case. Once the flash counts were totaled for each of the cases, an overall average was taken for the entire 60-minute period leading up to the tornado start time, identified as time 0. The next step was to plot time-series graphs of the same lightning characteristics with the help of SPSS for Windows. Plotting these graphs was helpful in allowing a quick assessment of the electrical changes taking place within the storms before, during, and after tornado touchdown. Graphs were completed for all 64 cases in each of the following categories: flash rate, percent positive, positive and negative peak currents, and multiplicity. Once complete, each case was analyzed for peaks, if any, in the lightning data. The term peak in this analysis is defined as the maximum value of a specific lightning characteristic most closely related to the tornado activity. It is important to note that that the average life cycle of a typical thunderstorm lasts approximately 60 minutes from cumulus to dissipating stage according to The Thunderstorm Report of 1949. The mature phase of a thunderstorm can last from 15-45 minutes depending on the intensity of the storm. Since the assumption was made that the tornadoes occurred during the mature phase of the thunderstorm, particular attention was paid to the time when maximum lightning activity could be expected; within a window of 30 minutes on either side of the tornado start time.

Table 4. Hourly flash rates and averages for F5 tornadoes.

time	case 74	case 75	case 76	case 77	case 78	F5 Total
-58	30	120	1020	690	480	468
-56	60	30	1110	810	510	504
-54	60	120	1590	810	540	624
-52	180	180	1380	480	480	540
-50	90	150	1290	480	330	468
-48	90	210	1500	570	180	510
-46	30	240	1770	660	270	594
-44	150	120	1890	1200	210	714
-42	30	90	1800	1320	210	690
-40	180	90	1890	870	420	690
-38	90	210	1560	840	540	648
-36	120	240	1830	720	660	714
-34	60	120	1650	540	480	570
-32	210	180	1380	810	360	588
-30	60	270	1620	660	510	624
-28	30	210	2640	810	480	834
-26	150	240	3180	960	840	1074
-24	150	330	2910	690	780	972
-22	240	360	3300	570	480	990
-20	210	330	2790	660	630	924
-18	480	390	3120	840	510	1068
-16	300	510	3390	570	420	1038
-14	180	330	3540	870	390	1062
-12	30	240	3810	930	300	1062
-10	60	270	3180	600	300	882
-8	30	270	2880	690	360	846
-6	0	420	3360	870	420	1014
-4	90	600	3900	510	240	1068
-2	180	420	3270	780	330	996
0	120	510	3210	570	360	954
Average Hourly Flash Count for F5 Tornadoes (Hour preceding tornado)						**791**

After average peak values and their time of occurrence were annotated, a table of

statistics was created for all storms based on intensity and season for the entire 2-hour

period centered the tornado start time. It should be noted that negative values of time

refer to the hour preceding tornado touchdown while positive values indicate time within

an hour after tornado occurrence. For each category of intensity or season, Statistix was

used to calculate the averages, confidence intervals, and standard deviations of the

desired lightning characteristics. The example shown in Table 5 is based on data used to

Table 5. Peak positive current and time of occurrence for F1 tornado events. Time of
occurrence is in reference to tornado start time. Negative times represents peak in
positive peak current before tornado touchdown.

Case number (F1 tornadoes)	Time of occurrence (minutes)	Peak positive current (kA)
1	-4	57
3	-7	90
4	-14	78
5	-7	80
6	-16	110
7	-24	20
8	-7	82
10	-26	50
11	-8	23
12	-14	40
14	-7	90
15	17	90
17	10	40
19	10	55

Table 6. Statistical overview of peak positive current for F1 tornado events. Time of occurrence is in reference to tornado start time. Negative times represents peak in positive peak current before tornado touchdown.

	Time	Current (kA)
LO 95% CI	-14.1	48.6
MEAN	-6.9	64.6
UP 95% CI	0.2	80.7
SD	12.4	27.7
MINIMUM	-26.0	20.0
1ST QUARTI	-14.5	40.0
3RD QUARTI	-0.5	90.0
MAXIMUM	17.0	110.0

calculate a statistical overview of peak positive current for F1 tornadoes. The descriptive statistics shown in Table 6 was the product of Statistix software. Comparisons were made between categories of intensity and season for all cases upon completion of the tables.

The statistical overview of Table 6 includes minimum and maximum values for peak positive current and time of occurrence within the data set. The first quartile includes 25 % of the sorted lightning data, and the third quartile includes 75 % of the sorted lightning data. The range between the first and third quartiles includes half of the data. In this example, average peak current for F1 tornado events was calculated to be 64.6 kA with an average time of peak current occurring at 6.9 minutes prior to tornado touchdown. The standard deviation of the averages explains how tightly all the data points are clustered around the mean in a set of data. A large standard deviation indicates a large amount of variability in the data while a small standard deviation indicates a small amount of variability. Finally, the 95 % upper and lower confidence interval (CI) implies that 95 % of all data points would be given within the interval that includes the population mean.

In general, the width of the confidence interval provides an idea about how much

uncertainty is associated with a specific parameter. A very wide interval **may** indicate

that more data should be collected before a final assessment can be made about the

parameter.

4. Results and Analysis

4.1 Overview

Chapter 3 provided details on how lightning data from 64 storm events were examined for unique signatures that may indicate the onset of tornadic activity. Characteristics were examined one hour prior and after tornado touchdown and divided into two categories based on storm intensity and seasonal variation. This chapter includes a synopsis of the characteristics studied along with the results of the research.

4.2 Summary of averages

4.2.1 Storm intensity

Flash rates were calculated for all storms and divided into categories based on storm intensity. The average flash rates for the storms are listed in Tables 7 and 8. Flash rates for the storms 60 minutes prior to tornado touchdown were lower than that of the flash rates for storms 60 minutes after tornado occurrence. An exception was noted for the F3 intensity storms where the flash rates actually decreased slightly after tornado touchdown. F4 and F5 storms showed significantly lower flash rates than the lower intensity tornadoes prior to tornado touchdown. This may be in part to the greater intracloud lightning activity associated with the more intense tornadoes. Verification of such activity would have required access to intracloud lightning data which was inaccessible during the time of the study.

Percentage of positive flashes were quite small in comparison to all CG flashes examined for all storms. For the F1-F3 intensity storms, the percent of positive flashes were slightly higher than that of the corresponding storms after tornado occurrence. F5

28

storms exhibited a slightly higher percentage of the positive flashes, accounting for about

20 percent of the CG flashes.

Table 7. Summary of lightning characteristics and their averages (One hour prior to tornado touchdown). A summary of lightning characteristics is provided in the table below for tornadoes of varying intensity. 2 minutes averages were calculated one hour prior up to the reported time of tornado occurrence.

Storm Intensity	Hourly Flash Rate	Percent Positive	Number of Flashes			Average Peak Current (kA)		Average Multiplicity	
			Pos	Neg	Total	Pos	Neg	Pos	Neg
F1	1064	8.8	3	32	35	21.2	-17.8	0.8	1.6
F2	890	13.8	4	25	29	16.1	-21.6	0.7	1.9
F3	1293	11.6	5	38	43	22.3	-20.7	1.0	2.0
F4	720	12.5	3	21	24	13.4	-21.4	0.7	1.9
F5	791	19.2	5	21	26	30.5	-18.9	1.1	1.8

Table 8. Summary of lightning characteristics and their averages (One hour after tornado touchdown). A summary of lightning characteristics is provided in the table below for tornadoes of varying intensity. 2 minutes averages were calculated from the reported time of tornado occurrence to one hour past .

Storm Intensity	Hourly Flash Rate	Percent Positive	Number of Flashes			Average Peak Current (kA)		Average Multiplicity	
			Pos	Neg	Total	Pos	Neg	Pos	Neg
F1	1121	8.1	3	34	37	21.1	-19.0	0.8	1.6
F2	943	12.9	4	27	31	19.4	-23.2	0.8	2.0
F3	832	11.1	3	24	27	22.6	-22.1	0.9	2.0
F4	1104	13.5	5	32	37	17.4	-22.8	0.9	2.0
F5	939	19.4	6	25	31	31.3	-17.7	1.1	1.8

Total number of flashes were higher for tornadic storms the hour after initial tornado touchdown. The only exception was a decrease, one hour after tornado touchdown, for F3 tornadoes. Overall, negative number of flashes were higher than positive flashes for all storms consistent with the results of the percent positive flashes.

Positive peak current remained about the same or showed a slight increase for all storms, before and after tornado touchdown, while the negative peak current showed decreases after tornado occurrence. The exception in the negative peak current was for the F5 tornadoes where an increase was noted. The range of positive peak currents varied from approximately 13 to 31 kA. The range for the negative peak current was smaller, ranging from –18 to –23 kA.

No significant differences between the multiplicity, both negative and positive, were seen throughout the study period for all tornado intensities.

4.2.2 Seasonal variations

Flash rates, percentage of positive flashes and number of CG flashes, positive and negative peak currents and multiplicity were compared for seasonal variations. Tables 9 and 10 summarize the characteristic findings.

Average CG flash rates showed some difference based on the time of year tornadoes occurred. Spring and summer flash rates were consistently higher than fall and winter. This may be in part to the different type of meteorological systems typically associated with these storms. The large number of storms in spring and summer in the United States could be the result of dryline interaction or mesoscale convective complexes. However, satellite data would be needed to prove this as the storm event data provided by the NCDC does not provide enough detail as to the origins of each storm.

Percent positive flashes showed seasonal patterns for both data sets prior to and after tornado occurrence. The highest percent positive flashes were seen one hour prior to tornado touchdown for summer and fall while fall and winter exhibited the highest percentages one hour after tornado touchdown. Negative flashes dominated all storms for all seasons. Peak currents were larger in magnitude for both positive and negative polarities one hour after the initial tornado report. Finally, positive and negative multiplicity showed no appreciable differences throughout the study period for all seasons.

Table 9. Summary of seasonal averages for all tornadoes (One hour prior to tornado touchdown). A summary of lightning characteristics for tornadic storms is provided by seasonal variations. 2 minutes averages were calculated one hour prior up to the reported time of tornado occurrence.

Season	Hourly Flash Rate	Percent Positive	Number of Flashes			Average Peak Current (kA)		Average Multiplicity	
			Pos	Neg	Total	Pos	Neg	Pos	Neg
Spring	870	12.8	4	25	29	17.8	-21.4	0.8	1.9
Summer	1326	8.4	4	40	44	21.5	-17.5	0.8	1.6
Fall	744	14.8	4	21	25	25	-18.8	0.8	1.6
Winter	807	16.8	5	22	27	16.2	-21.6	0.8	2.1

Table 10. Summary of seasonal averages for all tornadoes (One hour after tornado touchdown). A summary of lightning characteristics for tornadic storms is provided by seasonal variations. 2 minutes averages were calculated from the reported time of tornado occurrence to one hour past.

Season	Hourly Flash Rate	Percent Positive	Number of Flashes			Average Peak Current (kA)		Average Multiplicity	
			Pos	Neg	Total	Pos	Neg	Pos	Neg
Spring	1101	13.1	5	32	37	20.2	-22.8	0.9	2.0
Summer	1171	8.2	3	36	39	21.9	-19.4	0.8	1.7
Fall	490	18.9	3	14	17	25.3	-19.2	0.8	1.6
Winter	649	16.8	4	18	22	20.1	-24.2	0.9	2.0

4.3 Flash rates

4.3.1 Intensity based flash rates

Hourly flash rates were examined through time-series analysis with help of Excel, Statistix, and SPSS for Windows. Overall, 38 of the 64 storms displayed a distinct peak in hourly flash rates prior to reported tornado touchdown. Of those 38 cases, it was noted that approximately 53 % of the time the flash rates jumped to over 1000 flashes per hour before tornado occurrence. F3 tornadoes showed the greatest CG flash activity with 88 % of the storms exhibiting hourly flash counts over 1000 flashes per hour, prior to tornado occurrence. Figure 5 shows flash rates for an F4 tornado that struck Clifton, Tennessee. Flash rates increase sharply over 1000 flashes per hour about 18 minutes before tornado start.
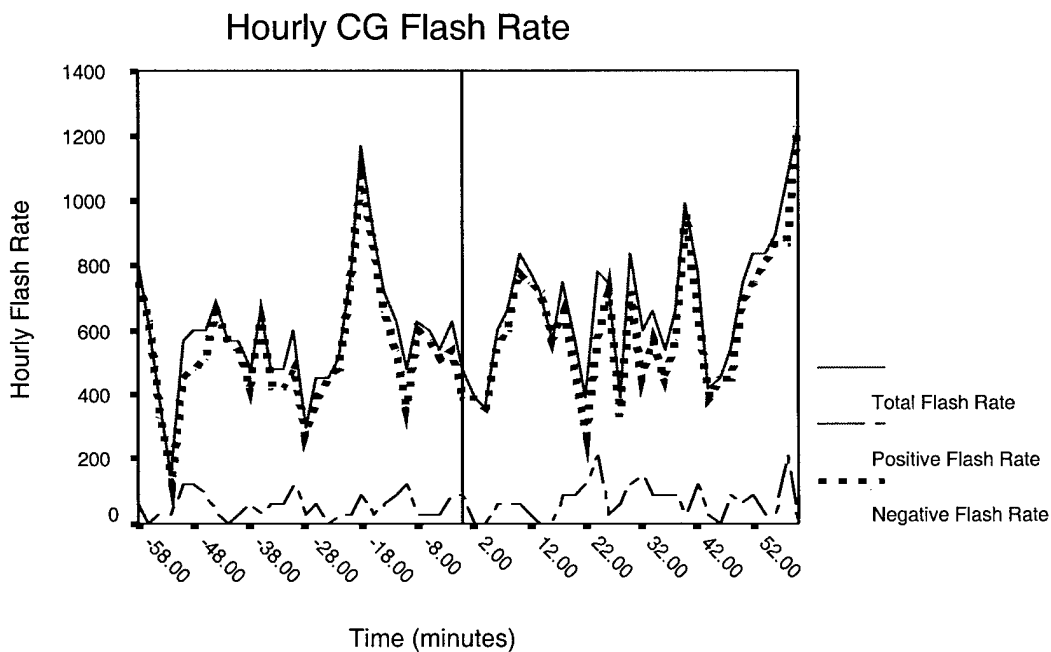

Figure 5. Hourly CG flash rates for the Clifton, TN tornado (F4) of April 16,1998. Note the distinct peak in the hourly flash rate approximately 15 minutes prior to tornado touchdown. The solid vertical line represents the reported tornado start time.

32

Table 11. Average flash rates for all intensity tornadoes. Average peak values for flash rates and time of occurrence were computed for tornadoes of all intensities (One hour prior to one hour after tornado start). Negative values for time represent occurrence prior to tornado. Min and max for peak flash counts and time are represented for all storm events in each intensity category.

Intensity		Low 95 % Confidence Interval	Mean	High 95 % Confidence Interval	Std Dev +/-	Min	Max
F1	Time (minutes)	-9.4	-3.8	1.7	10.0	-20.0	12.0
	Hourly Flash Rate	327	1585	2843	2271	60	7000
F2	Time (minutes)	-6.9	-3.0	0.9	7.6	-20.0	10.0
	Hourly Flash Rate	744	1304	1865	1090	120	4000
F3	Time (minutes)	-14.5	-6.5	1.4	13.2	-22.0	11.0
	Hourly Flash Rate	761	1467	2173	1168	225	3800
F4	Time (minutes)	-13.2	-4.8	3.6	13.2	-30.0	18.0
	Hourly Flash Rate	559	1175	1791	969	300	2800
F5	Time (minutes)	-25.6	-6.6	12.4	15.3	-24.0	16.0
	Hourly Flash Rate	558	1234	3026	1143	400	3800

The F1 and F2 tornadoes tended to show maximum CG flash rates approximately 1-3 minutes sooner than the intense F4-F5 tornadoes (Table 11). In addition, the average flash counts for F1-F3 tornadoes were slightly higher on average than the F4-F5 tornadoes. The lower counts could be a result of greater intracloud lightning activity in

these intense storms. The reduced flash count may also be the result of the limited

number of violent tornadoes available for examination in this case study.

4.3.2   Seasonal flash rates

Table 12. Average flash rates based on seasonal variations. Average peak values for
flash rates and time of occurrence were computed for tornadoes of all seasons (One hour
prior to one hour after tornado start). Negative values for time represent occurrence prior
to tornado. Min and max for peak flash counts and time are represented for all storm
events in each seasonal category.

Season		Low 95 % Confidence Interval	Mean	High 95 % Confidence Interval	Std Dev +/-	Min	Max
Spring	Time (minutes)	-6.0	-1.6	2.7	11.2	-30.0	18.0
	Hourly Flash Rate	914	1341	1768	1100	60	4000
Summer	Time (minutes)	-13.2	-8.0	-2.8	10.6	-22.0	10.0
	Hourly Flash Rate	711	1752	2793	2094	120	7000
Fall	Time (minutes)	-13.6	-2.3	8.9	10.7	-18.0	8.0
	Hourly Flash Rate	163	547	929	365	200	1000
Winter	Time (minutes)	-14.9	-7.3	0.3	10.6	-22.0	8.0
	Hourly Flash Rate	284	1050	1815	1070	200	3800

Spring and winter tornadoes showed the greatest hourly CG flash activity. CG flash

counts of 1000 flashes or greater accounted for approximately 56 % of the storm events

for each seasonal category, during the hour prior to tornado start.

Obvious seasonal trends were noted with respect to time and the occurrence of peaks

in the hourly flash rate (Figure 12). However, flash rates for fall and winter were

noticeably smaller than spring and summer. The small number of cases utilized for fall and winter may have had an influence on the overall flash rates for each of the seasonal categories. The standard deviations between all seasons showed very little spread. In fact, they were all within 1 flash per hour of one another.

4.4 Percent positive flashes

4.4.1 Intensity based percentage positive

No distinguishable trends were noted for most storms in the category of percent positive flashes. Only 9 of the 64 storm events were dominated by positive CG flashes during the entire time of study. Even more interesting was the total percentage of storms, only 29 %, showing crossover in polarity from positive to negative prior to the tornado start. The average time of polarity crossover for those few cases was found to be 9.2 minutes before reported tornado start. Figure 6 shows the lightning data for F5 tornado that decimated Oklahoma City on 3 May 1999. It was one of the few storm events examined that showed a dominate positive CG flash trend. The data shows a local maximum in percent positive flashes (~70 %) 10 minutes before tornado start with a slow decrease from that time till approximately 6 minutes after tornado start. Also, note the switch to negative polarity shortly after tornado start (percent positive drops below 50%).

Table 13 displays the average percent positive values and time of occurrence for tornadoes of all intensities. For all storms, except F3 intensity, the average time of peak percent positive CG activity was observed 1.5 - 4.5 minutes before tornado onset. The actual percent positive values showed only small difference between the intensity categories. Examination of the F5 value would give the impression that the most intense tornadoes exhibited a higher count of positive flashes than the rest of the storms.

35

Unfortunately, due to the small number of F5 storm events available, a total of 5, the

percentage of positive flashes calculate higher than the weaker intensity storms. This

result is due to the sensitivity of the mean to unusually large values in the data set.
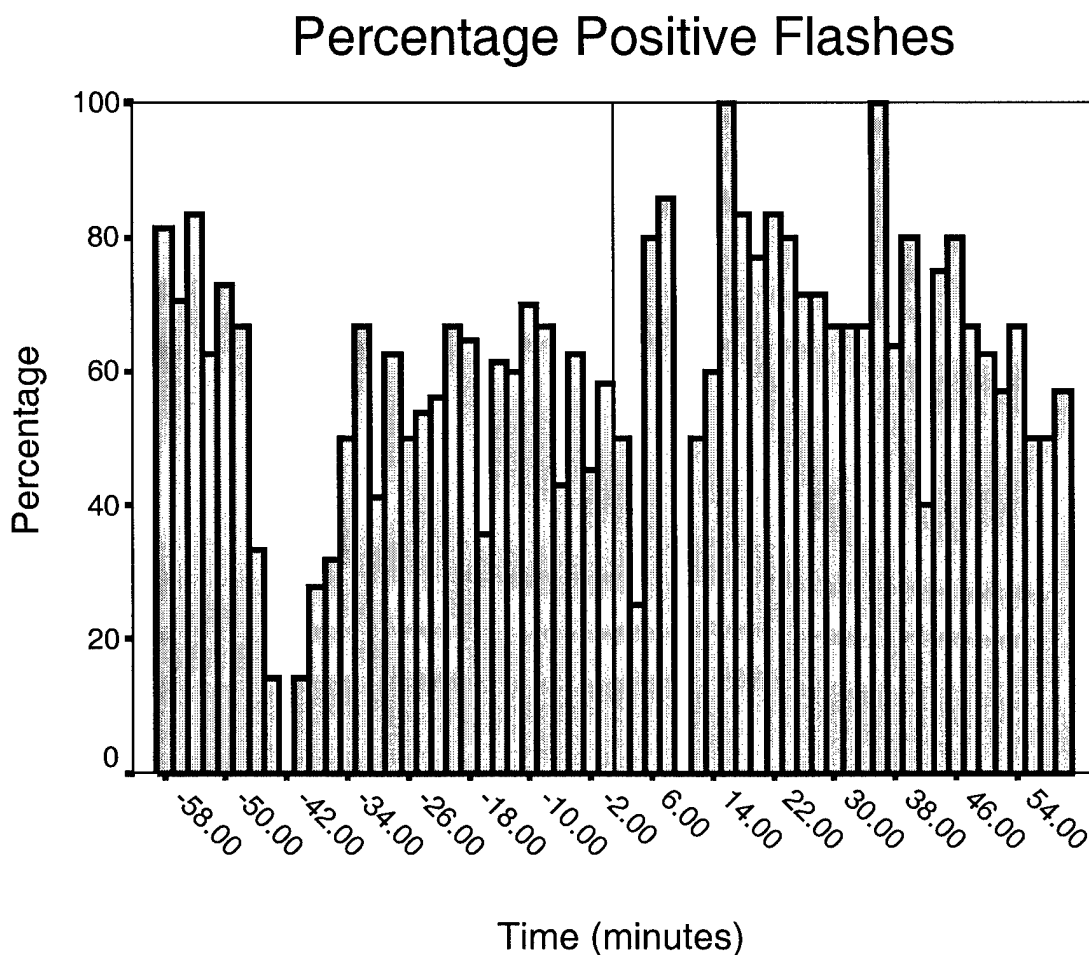
Percentage Positive Flashes

Figure 6. Percentage of positive flashes for the Oklahoma City tornado (F5) of
May 3, 1999. The storm associated with this tornado was primarily dominated by positive
flashes during the period of study. Solid vertical line represents reported tornado start
time.

Table 13. Average percent positive for all intensity tornadoes. Average percent positive flashes and time of occurrence were computed for tornadoes of all intensities (One hour prior to one hour after tornado start). Negative values for time represent occurrence prior to tornado. Min and max for peak flash counts and time are represented for all storm events in each intensity category.

Intensity		Low 95 % Confidence Interval	Mean	High 95 % Confidence Interval	Std Dev +/-	Min	Max
F1	Time (minutes)	-8.6	-3.4	1.8	9.4	-19.0	14.0
	% Positive	28	48	68	36	8	100
F2	Time (minutes)	-7.7	-4.5	-1.4	6.1	-16.0	6.0
	% Positive	23	39	56	33	9	100
F3	Time (minutes)	-5.2	1.1	7.4	10.9	-22.0	17.0
	% Positive	18	37	55	31	9	100
F4	Time (minutes)	-8.8	-4.4	0.0	7.3	-14.0	6.0
	% Positive	20	39	58	32	9	100
F5	Time (minutes)	-17.8	-1.4	15.0	13.2	-24.0	8.0
	% Positive	8	52	96	35	23	100

4.4.2 Seasonal percentage positive flashes

Summer showed the highest percentage of positive flash activity in the hour before tornado start, averaging 40 % (Table 14). This may due to the higher number of mesoscale convective complexes (MCCs) that frequent the United States during the summer months. Upper level wind shear associated with MCCs allows for a tilted charge

37

distribution (in the direction of cell movement) within the individual storm cells. The

resulting tilt may allow positive charge at the top of the storm a more direct path to

ground.

The average time for maximum positive CG flashes for all seasons was found to range

from 0 – 5 minutes before tornado onset. Overall positive flash counts showed only

small variations between seasons with nothing significant to note. Standard deviations for

summer and fall showed a larger variation, with respect to percentage positive flashes,

than spring and winter.

Table 14. Average percent positive based on seasonal variations. Average percent
positive flashes and time of occurrence were computed for tornadoes of all seasons (One
hour prior to one hour after tornado start). Negative values for time represent occurrence
prior to tornado. Min and max for peak flash counts and time are represented for all storm
events in each seasonal category.

Season		Low 95 % Confidence Interval	Mean	High 95 % Confidence Interval	Std Dev +/-	Min	Max
Spring	Time (minutes)	-5.8	-2.6	0.6	8.6	-19.0	16.0
	% Positive	25	35	45	27	5	100
Summer	Time (minutes)	-5.6	-1.0	3.6	9.2	-16.0	17.0
	% Positive	27	48	68	41	8	100
Fall	Time (minutes)	-12.2	-5.0	2.8	7.4	-12.0	8.0
	% Positive	13	52	91	37	25	100
Winter	Time (minutes)	-4.4	-0.1	4.1	5.5	-7.0	8.0
	% Positive	26	44	62	24	18	100

4.5 Average positive peak current

4.5.1 Intensity based positive peak current

All cases were examined to see if there were distinct peaks in the average of positive peak currents, especially before storm start time. The term "peak" refers to the maximum current in the first stroke of a lightning flash. 67 % of all storm events evaluated had their maximum before the onset of tornadic activity. Of those 40 cases, the average increase in peak current, from the previous two-minute current value to its maximum peak current value, was calculated to be 41 kA.
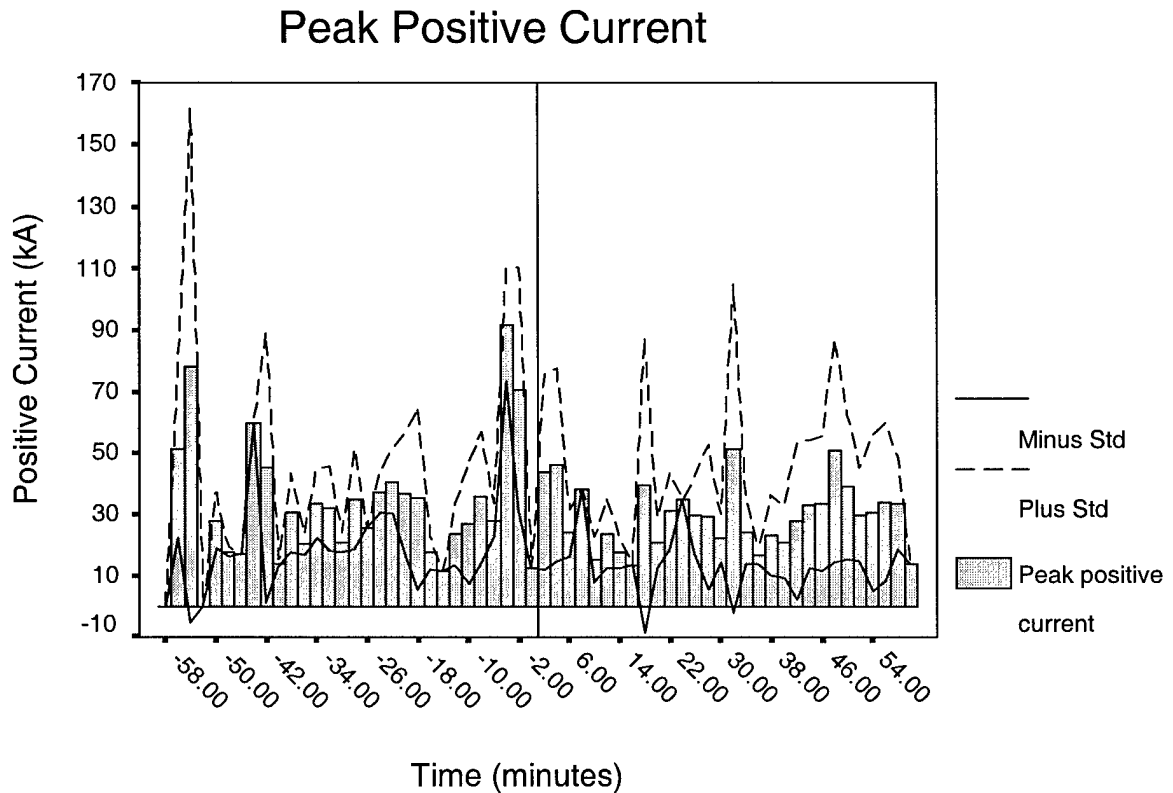
Figure 7. Time-series of positive peak current for the Nickelville, Georgia tornado (F1) that occurred November 11, 1995. Peak current shows a sharp increase just minutes before tornado touchdown. Upper and lower standard deviation lines are also included to show spread in the data for each 2-minute time increment. The zero value of positive peak current at ~52 minutes before tornado touchdown indicates that there were no positive CG flashes detected during that two-minute time increment. Solid vertical line represents reported tornado start time.

39

Figure 7 shows the time-series of positive peak current for a tornadic storm (F1) that occurred in Georgia in November of 1995. A distinct maximum in peak current was noted approximately 4 minutes prior to the storm start. This sharp increase in peak current can be verified by the spread of the standard deviation lines in Figure 7. During that time, average positive peak current jumped from 30 to 90 kA.

Table 15 breaks down the maximum peak current values for one hour prior out to one hour after tornado start. The weaker tornadoes, specifically the F1-F2 storms, showed an overall maximum in peak positive currents 3-5 minutes sooner than the more intense storms.

Table 15. Average peak positive current for all intensity tornadoes. Average peak current values for positive flashes and time of occurrence were computed for tornadoes of all intensities (One hour prior to one hour after tornado start). Negative values for time represent occurrence prior to tornado.

Intensity		Low 95 % Confidence Interval	Mean	High 95 % Confidence Interval	Std Dev +/-	Min	Max
F1	Time (minutes)	-14.1	-6.9	0.2	12.4	-26.0	17.0
	Positive Peak Current (kA)	48.6	64.6	80.7	27.7	20.0	110.0
F2	Time (minutes)	-9.7	-5.8	-1.8	7.7	-20.0	8.0
	Positive Peak Current (kA)	34.7	42.7	50.7	15.6	20.0	70.0
F3	Time (minutes)	-9.0	-1.3	6.5	12.1	-16.0	17.0
	Positive Peak Current (kA)	34.4	65.6	96.8	49.1	18.0	190.0
F4	Time (minutes)	-9.0	-2.9	3.1	9.5	-19.0	12.0
	Positive Peak Current (kA)	23.2	52.8	82.4	46.6	15.0	170.0
F5	Time (minutes)	-19.6	-3.0	13.6	13.4	-16.0	17.0
	Positive Peak Current (kA)	11.0	51.2	91.4	32.3	20.0	100.0

The average of the maximum peak currents varied by intensity, and did not reveal significant trends over time.

4.5.2 Seasonal positive peak current

The influence of seasonal variations on peak positive current was also investigated during this research. The summer and fall months exhibited the largest percentage of cases, 78 and 80 % respectively, with peaks in their positive current before tornado onset. Table 16 also indicates that during the summer and fall months average time of peak positive current hovered around 7 minutes before storm start. The only difference in seasonal positive peak current was noted for fall. Its current value was 30 kA higher than for all other seasons. The extremely small number of fall storm events included in this study, a total of 5, may account for the higher current values.

Table 16. Average peak positive current based on seasonal variations. Average peak current values for positive flashes and time of occurrence were computed for tornadoes of all seasons (One hour prior to one hour after tornado start). Negative values for time represent occurrence prior to tornado.

Season		Low 95 % Confidence Interval	Mean	High 95 % Confidence Interval	Std Dev +/-	Min	Max
Spring	Time (minutes)	-7.7	-3.0	1.7	12.1	-24.0	17.0
	Positive Peak Current (kA)	33.9	51.0	68.0	43.9	15.0	190.0
Summer	Time (minutes)	-10.7	-6.7	-2.6	8.2	-26.0	8.0
	Positive Peak Current (kA)	43.8	54.8	65.9	22.3	20.0	90.0
Fall	Time (minutes)	-21.4	-7.8	5.8	11.0	-20.0	8.0
	Positive Peak Current (kA)	33.5	82.4	131.3	39.4	27.0	125.0
Winter	Time (minutes)	-9.0	-1.8	5.4	9.3	-15.0	14.0
	Positive Peak Current (kA)	39.0	53.6	68.1	18.9	33.0	85.0

4.6 Average negative peak current

4.6.1 Intensity based negative peak current

Storm events were analyzed 60 minutes prior to and after the onset of tornadic

activity. Only 58 % of the storm events exhibited an extreme in negative peak currents

before tornado start as compared to 67 % seen for positive peak currents. The average

increase in current, from the previous two-minute current value to its maximum current

value, was also found to be much smaller, averaging 16 kA compared to 41 kA for
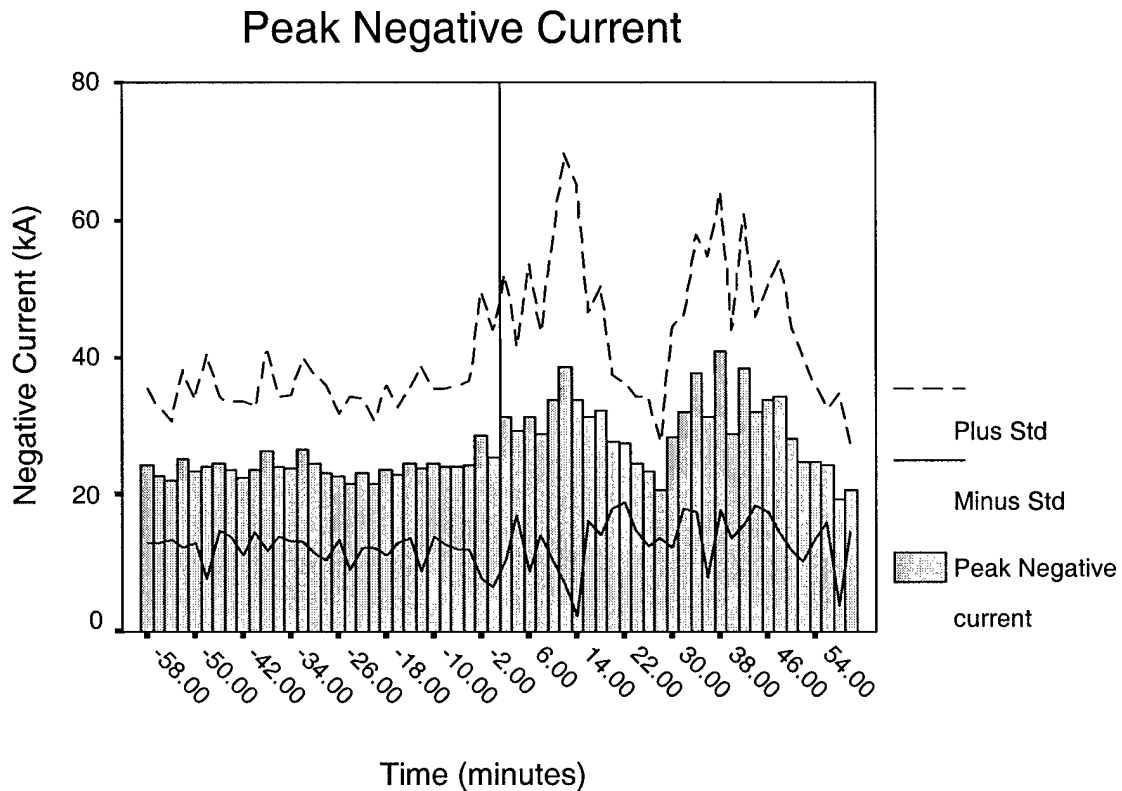
positive peak flashes.

Figure 8. Time-series of negative peak current for the Moscow, Ohio tornado (F3) of July 2, 1997. Note: The absolute value of the negative current is depicted. Upper and lower standard deviation lines are also included to show spread in the data for each 2-minute time increment. Solid vertical line represents reported tornado start time.

42

The tornadic storm, depicted in Figure 8, appears to have a maximum in negative peak current 12 minutes after tornado start. Closer examination of the data with standard deviations show that this may be misleading. Based on the spread of the standard deviation lines there is no substantial difference in the means of the peak negative current values. In general, for tornadoes of F3 intensity, percentage of cases showing a peak before or after storm commencement was split at 50 %. It should be noted that average negative peak current jumped in magnitude from -28 to –39 kA at that time.

Table 17. Average peak negative current for all intensity tornadoes. Average peak current values for negative flashes and time of occurrence were computed for tornadoes of all intensities (One hour prior to one hour after tornado start). Negative values for time represent occurrence prior to tornado.

Intensity		Low 95 % Confidence Interval	Mean	High 95 % Confidence Interval	Std Dev	Min	Max
F1	Time (minutes)	-12.7	-4.5	3.6	14.7	-31.0	16.0
	Negative Peak Current (kA)	-37.9	-31.8	-25.7	11.1	-60.0	-21.0
F2	Time (minutes)	-10.8	-2.8	5.2	14.4	-26.0	23.0
	Negative Peak Current (kA)	-42.8	-37.3	-31.9	9.8	-55.0	-23.0
F3	Time (minutes)	-9.0	-1.6	5.8	11.7	-20.0	12.0
	Negative Peak Current (kA)	-39.5	-32.6	-25.7	10.8	-58.0	-16.0
F4	Time (minutes)	-14.3	-4.8	4.6	14.8	-28.0	20.0
	Negative Peak Current (kA)	-37.9	-33.3	-28.7	7.2	-45.0	-22.0
F5	Time (minutes)	-14.9	-3.2	8.5	9.4	-12.0	12.0
	Negative Peak Current (kA)	-42.5	-28.4	-14.3	11.3	-48.0	-21.0

Overall, negative peak current showed little variation and averaged –32.7 kA for tornadoes of all intensities (Table 17). Time of maximum peak current values ranged from 1.6 minutes, for F3 tornadoes, to 4.8 minutes, for F4 tornadoes, before tornado onset. No further trends were noted for negative peak currents.

4.6.2 Seasonal negative peak current

Seasonal variations were observed for negative peak currents during the course of study. Spring and fall were the only seasons that had a majority of cases with peak negative current prior to tornadic activity. Less than 50 % of summer and winter cases

Peak Negative Current
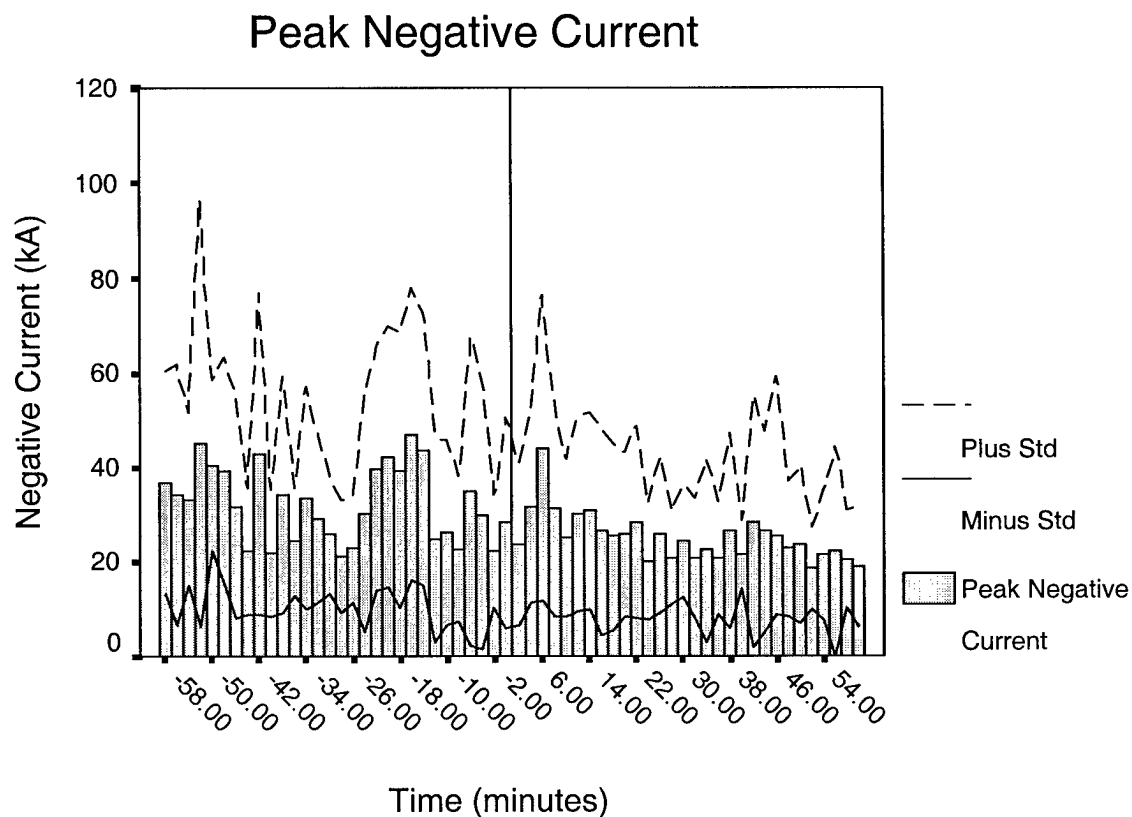

Figure 9. Time-series of negative peak current for a winter tornado. Winter storms spawned a tornado near Naylor, Arkansas, 21 January 1999. Note: The absolute value of the negative current is depicted. Upper and lower standard deviation lines are also included to show spread in the data for each 2-minute time increment. Solid vertical line represents reported tornado start time.

demonstrated this characteristic. Figure 9 depicts a winter storm event that shows two

maxima in negative peak current at 50 and 18 minutes before tornado start. Based on the

spread of the standard deviation lines at each of the times, there is no significant

difference in the means of the negative peak current values. Therefore, it can be

reasonably concluded that there are no significant maxima in negative peak current for

the entire storm event.

Table 18 demonstrates the variability in negative peak current and time of occurrence

between seasons. The standard deviation for time showed little variation between

seasons. However, the winter season displayed a rather interesting characteristic with its

Table 18. Average peak negative currents based on seasonal variations. Average peak
current values for negative flashes and time of occurrence were computed for tornadoes
of all seasons (One hour prior to one hour after tornado start). Negative values for time
represent occurrence prior to tornado

Season		Low 95 % Confidence Interval	Mean	High 95 % Confidence Interval	Std Dev	Min	Max
Spring	Time (minutes)	-7.9	-3.2	1.4	12.2	-28.0	20.0
	Negative Peak Current (kA)	-36.5	-33.0	-29.4	9.3	-60.0	-21.0
Summer	Time (minutes)	-10.8	-3.2	4.3	15.7	-31.0	14.0
	Negative Peak Current (kA)	-35.2	-30.9	-26.6	9.0	-55.0	-16.0
Fall	Time (minutes)	-27.6	-6.8	14.1	13.1	-22.0	10.0
	Negative Peak Current (kA)	-34.9	-26.5	-18.1	5.3	-34.0	-22.0
Winter	Time (minutes)	-10.2	0.0	10.2	13.3	-18.0	23.0
	Negative Peak Current (kA)	-50.5	-43.4	-36.4	9.2	-58.0	-29.0

45

overall average time of maximum negative peak current occurring at tornado start time.

This compared to almost 7 minutes before tornado start for the fall storm events. No

notable trends in data were found for average negative peak currents.

4.7 Multiplicity

4.7.1 Intensity based multiplicity

Positive Multiplicity
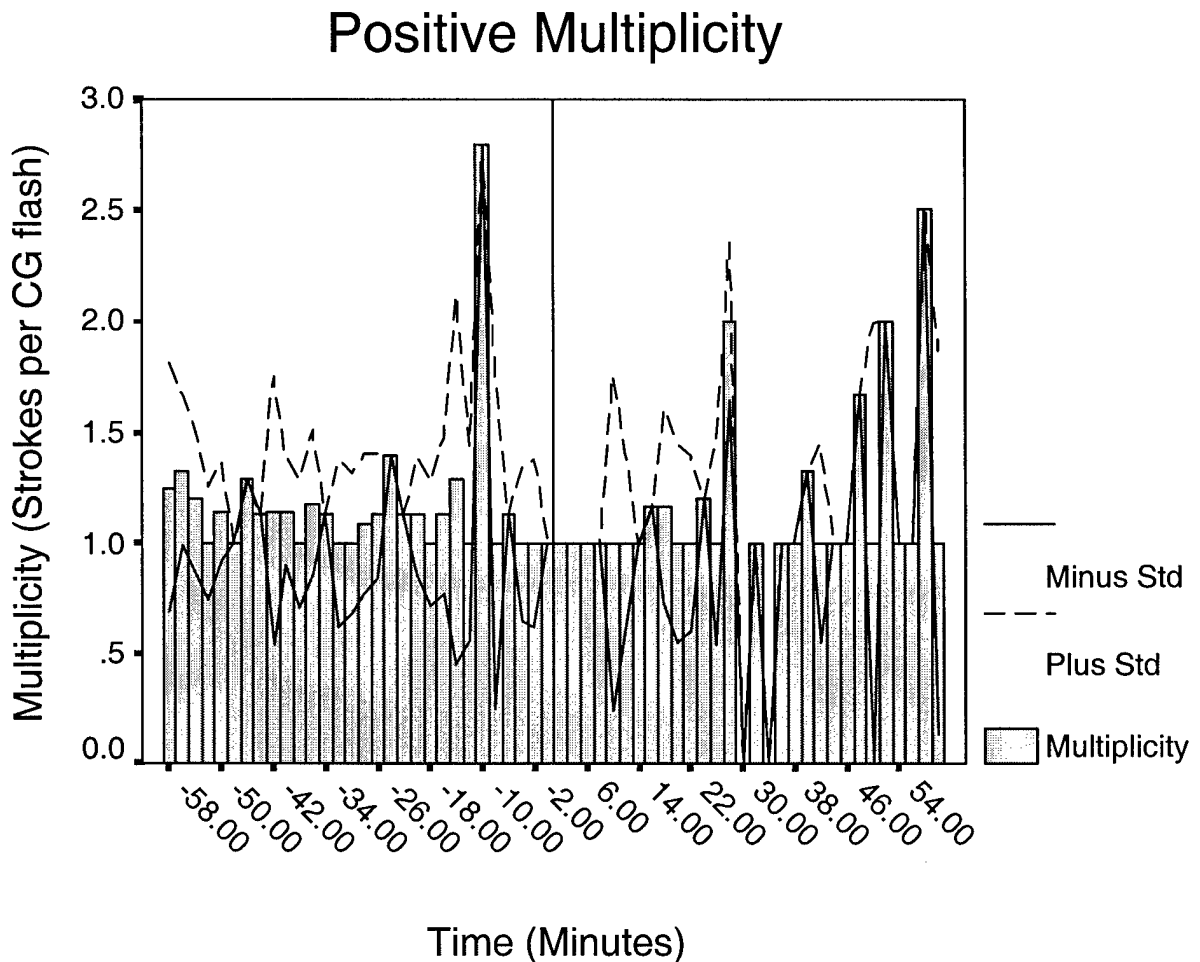
Figure 10. Plot of positive multiplicity for tornadic storm that struck Rome, Kentucky on January 3, 2000. Only 47 % of F3 tornadoes showed peak multiplicity prior to tornado onset. Upper and lower standard deviation lines are also included to show spread in the data for each 2-minute time increment. The zero values of positive multiplicity at ~32 and 34 minutes after tornado touchdown indicate that there were no positive CG flashes detected during those two-minute time increments. Solid vertical line represents reported tornado start time.

46

Multiplicity values for positive and negative flashes were analyzed with the help of time-series plots one hour and one hour after tornadogenesis. The storm event depicted in Figure 10 displayed relatively constant multiplicity rate with sharp increase approximately 15 minutes before tornado start. This maximum in multiplicity can be verified by examining the spread in the standard deviation lines in Figure 10. However, since there was only one positive CG flash for that two-minute time increment, it is difficult to justify this jump as a maximum in positive multiplicity. Multiplicity rates steadily increase again at the end of the study period possibly indicating redevelopment of thunderstorms in the vicinity. Average positive multiplicity at the maximum jumped by 1.5 strokes per flash, slightly higher than the average positive increase of 1.1 strokes, for all cases. Negative multiplicity had an overall higher average increase of 1.7 strokes.

Table 19 breaks down the specifics of the average multiplicity values. Overall, 60 % of storm events displayed a peak in multiplicity, both positive and negative polarities, one hour prior to tornado start.

Times for peak multiplicity for both positive and negative flashes showed quite a bit of variation with no obvious trends noted. Multiplicity values for positive CG flashes averaged around 1.9 for tornadoes of all intensities. In fact, the multiplicity values for the negative flashes hovered close to one another also, but the average was 3.0, slightly higher than for the positive values.

Table 19. Average multiplicity values for all intensity tornadoes. Average multiplicity values for positive and negative flashes and time of occurrence were computed for tornadoes of all intensities (One hour prior to one hour after tornado start). Negative values for time represent occurrence prior to tornado.

Intensity		Low 95 % Confidence Interval	Mean	High 95 % Confidence Interval	Std Dev	Min	Max
F1	Time (minutes)	-8.2	-2.7	2.8	10.0	-22.0	14.0
	Multiplicity (positive)	1.4	1.9	2.5	0.9	1.0	4.5
	Time (minutes)	-13.7	-6.6	0.5	12.8	-28.0	20.0
	Multiplicity (negative)	2.3	3.0	3.8	1.4	1.5	7.0
F2	Time (minutes)	-11.8	-1.7	8.4	16.7	-25.0	26.0
	Multiplicity (positive)	1.4	1.7	2.1	0.6	1.0	3.0
	Time (minutes)	-12.4	-5.1	2.2	14.2	24.0	20.0
	Multiplicity (negative)	2.8	3.2	3.6	0.8	2.3	5.0
F3	Time (minutes)	-8.9	0.3	9.5	15.2	-17.0	30.0
	Multiplicity (positive)	1.6	1.9	2.2	0.5	1.3	3.0
	Time (minutes)	-8.9	-0.7	7.5	14.3	-28.0	23.0
	Multiplicity (negative)	2.5	3.0	3.5	0.8	1.5	4.5

Table 19 continued.

Intensity		Low 95 % Confidence Interval	Mean	High 95 % Confidence Interval	Std Dev	Min	Max
F4	Time (minutes)	-13.9	-4.5	4.9	14.0	-20.0	18.0
	Multiplicity (positive)	1.4	1.9	2.4	0.8	1.2	3.5
	Time (minutes)	-11.3	-3.1	5.1	12.1	-18.0	20.0
	Multiplicity (negative)	2.5	2.9	3.2	0.5	2.1	3.4
F5	Time (minutes)	-25.2	-18.0	-10.8	4.5	-24.0	-14.0
	Multiplicity (positive)	0.7	2.2	3.6	0.9	1.5	3.5
	Time (minutes)	-17.5	1.8	21.0	12.1	16.0	10.0
	Multiplicity (negative)	1.3	2.7	4.1	0.9	1.6	3.7

4.7.2 Seasonal multiplicity variations

Time-series again was used to examine multiplicity values for both positive and negative flashes. For positive flashes, summer had the highest percentage of cases, 59 %, with a peak in multiplicity before tornado start. However, both summer and fall had the highest percentages, 65 % and 67 % respectively, for negative flashes. The summer storm event shown in Figure 11 was an exception to this, exhibiting little variation in multiplicity values throughout the time-series. The large spread in standard deviations for each two-minute time increment indicate little variation in the means throughout the time-series plot.
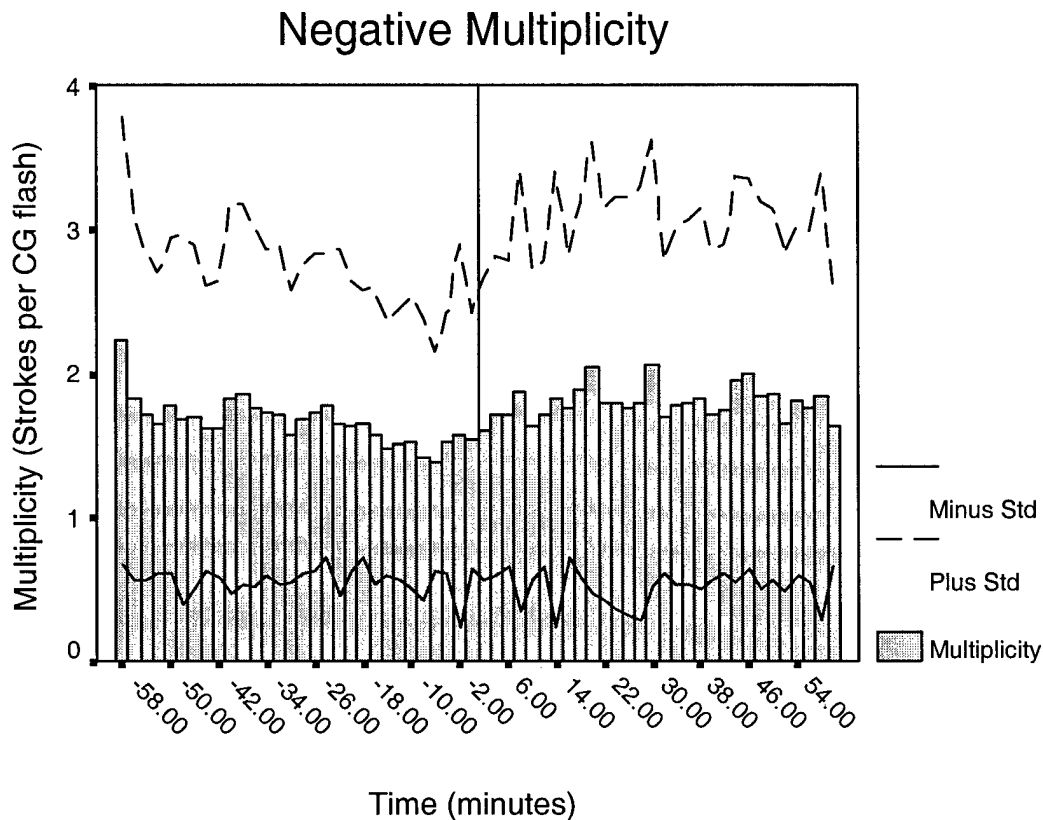
Figure 11. Negative multiplicity trace for summer storm event. This F1 tornado did minimal damage to Zanesville, Ohio on 27 June 1998. Upper and lower standard deviation lines are also included to show spread in the data for each 2-minute time increment. Solid vertical line represents reported tornado start time.

There is little difference between the multiplicity values found between the tornado intensity levels or seasonal variations. A look at Table 20 shows that times for peak multiplicity for both positive and negative flashes varied widely with no obvious trends noted. As with earlier results for intensities, the multiplicity values for positive CG flashes averaged around 1.9 for all seasons. Furthermore, the average multiplicity values for the negative flashes were also similar, hovering around 3.0 strokes per flash.

50

Table 20. Average multiplicity values based on seasonal variations. Average multiplicity values for positive and negative flashes and time of occurrence were computed for spring and summer (One hour prior to one hour after tornado start). Negative values for time represent occurrence prior to tornado.

Season		Low 95 % Confidence Interval	Mean	High 95 % Confidence Interval	Std Dev	Min	Max
Spring	Time (minutes)	-12.2	-7.1	-2.1	12.3	-25.0	15.0
	Multiplicity (positive)	1.6	1.9	2.3	0.8	1.0	4.5
	Time (minutes)	-7.5	-3.2	0.9	11.1	-26.0	20.0
	Multiplicity (negative)	2.8	3.1	3.5	1.0	2.0	7.0
Summer	Time (minutes)	-9.5	-1.7	6.1	14.1	-22.0	23.0
	Multiplicity (positive)	1.5	1.8	2.2	0.7	1.0	3.0
	Time (minutes)	-11.3	-3.4	4.3	15.2	-24.0	23.0
	Multiplicity (negative)	2.2	2.7	3.1	0.9	1.5	5.0
Fall	Time (minutes)	-20.9	0.8	22.5	17.4	-16.0	30.0
	Multiplicity (positive)	1.1	1.9	2.7	0.7	1.3	3.0
	Time (minutes)	-28.0	-9.7	8.7	17.5	-28.0	16.0
	Multiplicity (negative)	1.9	2.7	3.4	0.7	1.5	3.5
Winter	Time (minutes)	-10.5	0.2	10.9	15.0	-16.0	26.0
	Multiplicity (positive)	1.5	1.9	2.3	0.6	1.3	3.0
	Time (minutes)	-12.1	-1.2	9.6	14.1	-21.0	20.0
	Multiplicity (negative)	3.0	3.5	4.1	0.8	2.5	4.7

5. Conclusions

5.1 Conclusions

Cloud-to-ground lightning characteristics of 64 tornadic storms were examined over a five-year period to identify possible lightning signatures indicative of tornadic development. Based on the results of this research, there is little evidence to support the theory that specific lightning trends emerge prior to tornadogenesis.

Due to the inconsistent and unreliable nature of the results, exclusive use of this time-series technique is not recommended for use in operational forecasting. The use of conventional methods, such as radar and/or satellite, used in conjunction with cloud-to-ground lightning flash data may, however, provide insight as to how electrical and physical changes relate to the development of tornadoes within a storm. Intracloud lightning may also provide additional information on tornado development and should be included in future research projects, if the data is available.

5.2 Summary of results

The results of hourly flash rates for all storm events showed only a little over 50% of the tornadic storms displayed a distinct peak in hourly flash rates within 30 minutes of tornado touchdown. Of those storms, just over half exhibited flash rates of over 1000 flashes per hour. This trend may be the result of rapid intensification of the severe thunderstorm just prior to the tornado. In-depth storm analysis with the help of radar and satellite is necessary to investigate how the storm structure changes before rotation develops.

Only 9 of the 64 storm events were dominated by positive CG flashes. In fact, out of the 64 storm events examined, only 29 % of the storms showed crossover in polarity from

positive to negative prior to tornado start. The average time of observed crossover occurred approximately 9.2 minutes before tornado touchdown. F5 tornadoes exhibited the highest percent positive flashes based on intensity. This result should be viewed cautiously as it may not truly represent physical changes in storm structure, but may rather be due to the limited number of F5 cases utilized in the study. Summer storms had the highest percentage of positive flash activity in the hour before tornado occurrence. The higher frequency of mesoscale convective complexes found in the United States during the summer months may explain the increased number of positive CG flashes observed.

More than half of all storm events studied showed a maximum in their peak current before the onset of tornadic activity. The number of cases with a negative peak current maximum before tornado start accounted for 58 % of all storm events compared to 67 % seen for positive peak currents. It was also found that the average increase in current, from the previous two-minute current value to its maximum current value averaged 16 kA for negative flashes and 41 kA for positive flashes. Seasonal variations were not found to be significant factors for differences in peak currents.

The percentage of storms exhibiting peak multiplicity values before tornado onset varied by intensity and season. However, multiplicity values for both positive and negative flashes maintained the same values regardless of intensity or season. Average peak multiplicity values for positive flashes were 1.9 strokes per flash. Peak multiplicity values for negative flashes were slightly higher at 3.0 strokes per flash.

5.3 Recommendations for future research

First and foremost, all of the work accomplished in this study should be duplicated for non-tornadic storm events. It would be worthwhile to see if the trends found in this study are common in <u>all</u> thunderstorms or just materialize in tornadic thunderstorms.

Use of radar overlays would be beneficial in examining physical changes taking place in severe thunderstorms and how they relate to changes in lightning trends. This is particularly important because changes in severe thunderstorms are often rapid and sometimes unpredictable. Suggestions of areas to focus on include, but are not limited to, storm tops, hail activity, and storm rotation. Information about storm tops could assist in evaluating how storm intensity changes over time. Correlation between the presence of hail and peak or lulls in lightning activity could be explored. This may provide insight as to how charge is distributed and eventually transferred within the storm. Peak in lightning activity, i.e. flash rates, as it relates to the development of mesoscale rotation within the storm could be useful in determining whether tornado development is imminent.

Future research with spatial analysis could also be of help in determining relationships between CG flashes and tornado path. This could be accomplished by writing a program that plots all existing CG lightning flashes along with a plot of tornado path. Relationships between lightning activity with respect to distance and direction of tornadoes could be analyzed and compared for similarities and differences.

In the future, it would be of help to have access to intracloud lightning data to further investigate lightning trends in tornadic thunderstorms. At this time, NASA utilizes the Lightning Imaging Sensor (LIS) on the Tropical Rainfall Measuring Mission (TRMM) satellite to record intracloud flash rates as the satellite passes over a location (Strickler

54

and Phillips, 2000). Unfortunately, TRMM only provides a 90 second snapshot of lightning activity as it passes over. Ideally, the instruments must be moved to a geosynchronous orbit in order to observe intracloud activity continuously. This project is currently being pursued by NASA and should have the full support of the United States Air Force.

Appendix A. IDL programming code.

Appendix A. contains IDL programming code for **readfile.pro** and

histogramdata.pro programs discussed in Section 3.3.1

The first program written, **readfile.pro**, accessed the NLDN lightning data stored

on the local server at AFIT and saved it to a designated file for each individual storm

event. The next program, **histogramdata.pro,** read data from the previously created files

from the **readfile** program and calculated average positive and negative flash count, peak

current, and multiplicity for a time increment specified by the user.

Readfile.pro

```
pro readfile    ; reads data from existing file

;how many cases (lines of code) are in file
s=' '
n=0
openr,lun,'caselist.txt',/Get_lun
while not (eof(lun)) do begin
readf,lun,s
n=n+1
endwhile
close,lun

;convert numbers into string
num=strcompress(sindgen(100),/remove_all)
num[0:9]='0'+num[0:9]   ;gives two-digit strings

;read data

mon1=0
day1=0
yr1=0
hr1=0
min1=0
sec1=0

mon2=0
day2=0
yr2=0
hr2=0
min2=0
sec2=0

minlat=0.0
maxlat=0.0
minlon=0.0
maxlon=0.0

;open file and read data from file

file='   '
openr,lun,'caselist.txt',/Get_lun

for i=0, n-1 do begin
readf, lun,mon1,day1,yr1,hr1,min1,sec1,mon2,day2,yr2,hr2,min2,sec2,$
```

```
minlat,maxlat,minlon,maxlon
print,i+1,' of', n

isolate_data,dates=[num(mon1)+'/'+num(day1)+'/'+num(yr1)+'
'+num(hr1)+':'+num(min1)+':'+num(sec1) ,$
num(mon2)+'/'+num(day2)+'/'+num(yr2)+' '+num(hr2)+':'+num(min2)+':'+num(sec2)], $
region=[minlat,maxlat,minlon,maxlon],file='/home/kramer3/users/wseaman/lightningpro
grams/thesisdata/case'+num(i+1),/ascii,/overwrite

endfor
close,lun
free_lun,lun
end
```

Histogram.pro

```
pro histogramdata    ; calculated average positive and negative flash count, peak current,
; and multiplicity for a specified time increment

;how many cases are in file
s=' '
q=0
openr,lun,'caselist.txt',/Get_lun
while not (eof(lun)) do begin
readf,lun,s
q=q+1
endwhile
close,lun

;convert numbers into string
num=strcompress(sindgen(100),/remove_all)
num[0:9]='0'+num[0:9]   ;gives two-digit strings

cat='/home/kramer3/users/wseaman/lightningprograms/thesisdata/'

;open each file and read in lightning data
 for i=1, q do begin
        print,i,' of', q
        ; check to see if file exists
        test = findfile(cat+'case'+num(i)+'.lgh', count = count)

              if(count GT 0) then begin

              openr,lun,cat+'case'+num(i)+'.lgh',/Get_lun
              a=fstat(lun) ;gives information about file size
              n=a.size/11   ; tells number of flashes per file (11 bytes per flash)
              f=bytarr(11,n) ; creates a 2-d array
              readu,lun,f ; reads unformatted binary data from a file into IDL variables
              close,lun
              f=exp_lgh(f) ;converts binary data stored by .lgh file into a structure with
                    ;individual lightning components

        ;elapsed time from start
        month=0
        day=0
        year=0
        hour=0
        minute=0
        second=0
```

```
;read in data from reference time file
openr,lun,'reftime.txt',/Get_lun
        for j=1, i do begin
        readf,lun,month,day,year,hour,minute,second
        endfor
        close,lun
        free_lun,lun

;converts selected ref time to julian date
tref=julday(month,day,year,hour,minute,second)
time=dblarr(n) ;time as double precision floating point

        for k=0L,n-1 do begin
        ; converts computer's date to julian date
        time[k]=julday(f[k].month,f[k].day,f[k].year,f[k].hour,f[k].minute,$
        f[k].second)
        endfor
        time=time-tref

; only keep flashes after tref
keep=where (time GE 0.0, n)
if (n GT  0) then begin
f=f(keep)
time=time(keep)
time1=time*1440.0 ; converts time from days to minutes
endif


;isolate flashes and place into appropriate bins
dt=2.0
tbin=time1/dt ; tells what bin flash data goes into
tbinf=fix(tbin)
time1f=fix(time1)

        bin=tbin[n-1]+1  ; tells how many bins are needed with size dz
        pos=fltarr(bin) ;sets up array with size "tbin"
        neg=fltarr(bin) ;sets up array with size "tbin"
        multp=fltarr(bin);sets up array with size "tbin"
        multn=fltarr(bin);sets up array with size "tbin"
        counterp=fltarr(bin);sets up array with size "tbin"
        countern=fltarr(bin);fltarr(bin);sets up array with size "tbin"
        posfloat=fltarr(bin)
        negfloat=fltarr(bin)
        multpfloat=fltarr(bin)
        multnfloat= fltarr(bin)
        counterpfloat= fltarr(bin)
```

```
                            counternfloat= fltarr(bin)
                            avgpeakp= fltarr(bin)
                            avgpeakn= fltarr(bin)
                            avgmultp= fltarr(bin)
                            avgmultn= fltarr(bin)

        for l= 0, n-1 do begin

                            if f[l].peak GE 10.0 then begin
                            ; keep track of # of positive flashes
                            counterp[tbinf[l]]=counterp[tbinf[l]]+1
                            ;puts positive peak current in appropriate bin and sum them
                            pos[tbinf[l]]=pos[tbinf[l]]+f[l].peak
                            ;puts  pos multiplicity in appropriate bin and sums them
                            multp[tbinf[[l]]=multp[tbinf[[l]]]+f[l].mult
                            endif

                            if f.peak LT 0.0 then begin
                            ; keep track of # of negative flashes
                            countern[tbinf[l]]=countern[tbinf[l]]+1
                            ;puts negative peak current in appropriate bin and sum them
                            neg[tbinf[l]]=neg[tbinf[l]]+f[l].peak
                            ;puts neg multiplicity in appropriate bin and sums them
                            multn[tbinf[[l]]=multn[tbinf[[l]]]+f[l].mult
                            endif
        endfor


                            ;converts all sums to floating decimal point
                            counterpfloat=float(counterp)
                            counternfloat=float(countern)
                            posfloat=float(pos)
                            negfloat=float(neg)
                            multpfloat=float(multp)
                            multnfloat=float(multn)

dog='/home/kramer3/users/wseaman/lightningprograms/'
openw,outfile,dog+'histogram'+num( i ) +'.txt',/Get_lun, width=100
a='time  countp    avg pcur    avg pmult    countn   avg ncur   avg nmult'
printf, outfile,a

increment= 2.0 :minutes
for avg=0, bin-1  do begin

        if(counterpfloat[avg]  GT 0.0) then begin
                ;calculates average positive peak current per time
```

61

```
            avgpeakp[avg]=posfloat[avg]/counterpfloat[avg]
            ;calculates average positive multiplicity per time
            avmultp[avg]=multpfloat[avg]/counterpfloat[avg]

    endif


    if(counternfloat[avg]  GT 0.0) then begin
            ;calculates average negative peak current per time
            avgpeakn[avg]=negfloat[avg]/counternfloat[avg]
            ;calculates average negative multiplicity per time
            avmultn[avg]=multnfloat[avg]/counternfloat[avg]

    endif

    printf,outfile,fix(dt), fix(counterpfloat[avg],' ', avgpeakp[avg],' ', $
    avgmultp[avg], '  ',fix(counternfloat[avg],' ', avgpeakn[avg],' ', $
    avgmultn[avg]

    dt=dt+1
    endfor

            close, outfile
            Free_lun,outfile


        endif
endfor

    end
```

Bibliography

Branick, M.L., and C.A. Doswell III, 1992: An observation of the relationship between supercell structure and lightning ground-strike polarity. *Wea Forecasting*, **7**, 143-149.

Cummins K., M.J. Murphy, E.A. Bardo, W.L. Hiscox, R.B.Pyle, and A.E. Pifer, 1998: A combined TOA/MDF technology upgrade of the U.S. National Lightning Detection Network. *J. Geophys. Res.*, **103**, 9035-9044.

Curran, E.B., and W. D. Rust, 1992: Positive ground flashes produced by low-precipitation thunderstorms in Oklahoma on 26 April 1984. *Mon. Wea. Rev.*, **120**, 544-553.

Elson, D. B., 1993: Relating cloud-to-ground lightning to severe weather in Indiana on 2 June 1990. *Natl. Wea. Dig*, **18**, 15-19.

Fujita T. T., 1981: Tornadoes and downbursts in the context of generalized planetary Scales. *J. Atmos. Sci.*, **38**, 1511-1534.

Holle, R.L., and P.E. Lopez, 1993: Overview of real-time lightning detection systems and their meteorological uses. *NOAA Technical memorandum ERL NSSL-10. National Severe Storms Laboratory, Norman, OK*, 1-68.

Jones, H.L., 1951: A sferic method of tornado identification and tracking. *Bull. Amer. Meteor. Soc.*, **32,** 380-385.

Kane, R. J., 1991: Correlating lightning to severe local storms in the northeastern United States. *Wea Forecasting*, **6**, 3-12.

Knapp, D. I., 1994: Using cloud-to-ground-lightning data to identify tornadic thunderstorm signature and nowcast severe weather. *Natl. Wea. Dig*, **19**, 35-42.

Kohl, D.A., 1962: Sferics amplitude distribution jump identification of a tornado event. *Mon. Wea. Rev.*, **90**, 451-456.

MacGorman, D.R., V.M. Mazur, W.D. Rust, W.L. Taylor, and B.C. Johnson, 1989: Lightning rates relative to tornadic storm evolution on 22 May 1981. *J. Atmos. Sci.*, **46**, 221-250.

MacGorman, D.R., and D.W. Burgess, 1994: Positive cloud-to-ground lightning in tornadic storms and hailstorms. *Mon. Wea. Rev.*, **122**, 1671-1697.

Maier, M.W., and E.P. Krider, 1982: A comparative study of cloud-to-ground lightning characteristics in Florida and Oklahoma thunderstorms. *Preprints: Twelfth Conference on Severe Local Storms,* San Antonio, Texas, Amer. Meteor. Soc., 334-337.

National Climatic Data Center. NCDC storm events database. n.pag. http://www4.ncdc.noaa.gov/cgi-win/wwcgi.dll?wwEvent~Storms. 1 Sep 2000.

Perez, A.H., L.J. Wicker, and R.E. Orville, 1997: Characteristics of cloud-to-ground lightning associated with violent tornadoes. *Wea Forecasting*, **12**, 428-437.

Seimon, A., 1993: Anomalous cloud-to-ground lightning in an F5-tornado-producing supercell thunderstorm on 28 August 1990. *Bull. Amer. Meteor. Soc.*, **74**, 189-203.

Strickler, A. and T. Phillips. "Spotting Tornadoes from Space." Excerpt from article. n. pag. http://science.nasa.gov/headlines/y2000/ast01may_1m.htm. 1 May 2000.

Turman, B.N., and R.J. Tettlebach, 1980: Synoptic-scale satellite lightning observations in conjunction with tornadoes. *Mon. Wea. Rev.,* **108**, 1878-1882.

Wallace, J. M. and P. V. Hobbs, Atmospheric Science: An Introductory Survey. New York: Academic Press, 1977.

Uman, M. A., The Lightning Discharge. Orlando: Academic Press, 1987.

United States Department of Commerce. The Thunderstorm: Report of the thunderstorm project. Washington: GPO, 1949.

Vonnegut, B., 1960: Electrical theory of tornadoes. *J. Geophys. Res.,* **65**, 203-212.

Vita

Captain Wendy L. Seaman was born in Passaic, New Jersey. She graduated from Saddle Brook High School in Saddle Brook, New Jersey in June, 1986. Shortly after graduation, she entered the United States Air Force and was trained as a Weather Equipment Specialist. She served at Kelly AFB, San Antonio, Texas until January, 1990. She entered the undergraduate meteorology program at North Carolina State University in Raleigh, North Carolina where she graduated Cum Laude in December, 1996. Upon graduation, she was commissioned as a 2nd Lieutenant through Detachment 595 AFROTC at North Carolina State University.

Captain Seaman's first officer assignment was to Hill AFB in Ogden, Utah where she served as a Wing Weather Officer for the 75th Operational Support Squadron. She provided briefing support for the 388th and 419th Fighter Wings, 151st Air Refueling Wing, and the 1st Battalion/211th Aviation Brigade to name a few. In August 1999, she entered the graduate meteorology program at the Air Force Institute of Technology, School of Engineering and Management, at Wright-Patterson AFB, Dayton, Ohio. Upon graduation, Captain Seaman will be assigned to USAFE OWS, Sembach ABS, GE.

REPORT DOCUMENTATION PAGE

The public reporting burden for this collection of information is estimated to average 1 hour per response, including the time for reviewing instructions, searching existing data sources, gathering and maintaining the data needed, and completing and reviewing the collection of information. Send comments regarding this burden estimate or any other aspect of the collection of information, including suggestions for reducing this burden to Department of Defense, Washington Headquarters Services, Directorate for Information Operations and Reports (0704-0188), 1215 Jefferson Davis Highway, Suite 1204, Arlington, VA 22202-4302. Respondents should be aware that notwithstanding any other provision of law, no person shall be subject to an penalty for failing to comply with a collection of information if it does not display a currently valid OMB control number.
PLEASE DO NOT RETURN YOUR FORM TO THE ABOVE ADDRESS.

1. REPORT DATE (DD-MM-YYYY) 05-03-2001	2. REPORT TYPE Master's Thesis	3. DATES COVERED (From – To) Aug 2000 – Mar 2001

4. TITLE AND SUBTITLE

EVOLUTION OF CLOUD-TO-GROUND LIGHTNING DISCHARGES IN TORNADIC THUNDERSTORMS

5a. CONTRACT NUMBER

5b. GRANT NUMBER

5c. PROGRAM ELEMENT NUMBER

6. AUTHOR(S)

Seaman , Wendy, L., Captain, USAF

5d. PROJECT NUMBER

5e. TASK NUMBER

5f. WORK UNIT NUMBER

7. PERFORMING ORGANIZATION NAMES(S) AND ADDRESS(S)

Air Force Institute of Technology
Graduate School of Engineering and Management (AFIT/EN)
2950 P Street, Building 640
WPAFB OH 45433-7765

8. PERFORMING ORGANIZATION REPORT NUMBER

AFIT/GM/ENP/01M-07

9. SPONSORING/MONITORING AGENCY NAME(S) AND ADDRESS(ES)

Lt. Col Mark P. Weadon
88th Weather Squadron
WPAFB OH 45433-7765   DSN: 785-2207

10. SPONSOR/MONITOR'S ACRONYM(S)

11. SPONSOR/MONITOR'S REPORT NUMBER(S)

12. DISTRIBUTION/AVAILABILITY STATEMENT

APPROVED FOR PUBLIC RELEASE; DISTRIBUTION UNLIMITED.

13. SUPPLEMENTARY NOTES

14. ABSTRACT

Air Force operations are directly impacted by weather on a daily basis. Erroneous forecasts negatively impact mission readiness and consequently cost the government time, in terms of wasted man-hours, and money. Advanced forecast lead-time could make a difference to minimize loss to both USAF personnel and assets.

This study examined lightning data from 64 storm events from 1995-2000 in search of unique lightning signatures indicative of tornadic activity. Overall flash rates, percentage of positive flashes, positive and negative peak currents and multiplicity for each case were separated into two categories based on tornado intensity and season of occurrence. Based on the research results, there is little evidence to support the theory that specific lightning trends emerge prior to tornadogenesis.

Due to the inconsistent and unreliable nature of the results, exclusive use of this time-series technique is not recommended for use in operational forecasting. The use of conventional methods, such as radar and/or satellite, used in conjunction with cloud-to-ground lightning flash data may, however, provide insight as to how electrical and physical changes relate to the development of tornadoes within a storm. Intracloud lightning may also provide additional information on tornado development and should be included in future research projects.

15. SUBJECT TERMS
Lightning, Cloud-to-Ground Lightning, Tornadoes

16. SECURITY CLASSIFICATION OF:			17. LIMITATION OF ABSTRACT	18. NUMBER OF PAGES	19a. NAME OF RESPONSIBLE PERSON Maj. Gary Huffines, ENP
a. REPORT U	b. ABSTRACT U	c. THIS PAGE U	UU	76	19b. TELEPHONE NUMBER (Include area code) Enter Advisors Information (Example: (937) 255-3636, ext 1234) 937-255-3636 ext. 4511 (DSN 785-3636 ext. 4511)

Standard Form 298 (Rev. 8-98)
Prescribed by ANSI Std. Z39-18